Circuit structural plasticity by a neurotrophin with a Toll modifies behaviour

Jun Sun[1], Suzana Ulian-Benitez[1,2], Manuel G. Forero[3], Guiyi Li[1], Deepanshu Singh[1], Francisca Rojo-Cortés[1], Xiaocui Wang[1], Sebastian Cachero[4], Marta Moreira[1], Dean Kavanagh[5], Gregory Jefferis[4], Vincent Croset[6], and Alicia Hidalgo[1*]

1, Structural Plasticity & Regeneration Group, School of Biosciences, University of Birmingham, UK;

2, Current address: Buck Institute for Research on Aging, California, US;

3, Semillero Lún, Grupo D+Tec, Universidad de Ibagué, Colombia;

4, MRC LMB, Cambridge, UK;

5, Institute of Biomedical Research, University of Birmingham, UK.

6, Department of Biosciences, Durham University, UK.

*Author for correspondence:

00 44 (0)121 4145416

a.hidalgo@bham.ac.uk

Short running title: Novel mechanism of structural plasticity that modulates behaviour reveals how activity shapes the brain.

Keywords: Drosophila, plasticity, brain plasticity, structural plasticity, synaptogenesis, dendritic branching, neurodegeneration, long-term memory, locomotion, neuronal activity, dopamine, neurotrophin, DNT-2, Toll, Toll-6, Kek-6, Toll-Like Receptor, Kekkon, Kek, TrkB, TrkB-T1, TrkC-T1

ABSTRACT

Experience shapes the brain, as neural circuits can be modified by neural stimulation or the lack of it. How this modifies behaviour, and the underlying molecular mechanisms, are poorly understood, but could reveal how the brain works, in health and disease. Subjective experience requires dopamine, a neuromodulator that assigns a value to stimuli, and it also controls behaviour, including locomotion, learning and memory. In Drosophila, Toll receptors are ideally placed to translate experience into structural brain change. *Toll-6* is expressed in dopaminergic neurons (DANs), raising the intriguing possibility that Toll-6 could regulate structural plasticity in dopaminergic circuits. Drosophila neurotrophin-2 (DNT-2) is the ligand for Toll-6, but whether it is required for circuit structural plasticity was unknown. Here, we show that *DNT-2* expressing neurons are connected with DANs and they modulate each other. Loss of function for *DNT-2* or its receptors *Toll-6* and kinase-less Trk-like *kek-6* caused DAN and synapse loss, impaired dendrite growth and caused locomotion deficits. By contrast, over-expressed *DNT-2* increased dendrite complexity and promoted synaptogenesis. Neuronal activity increased the levels of DNT-2 and its maturation, and induced synaptic remodelling, which required *DNT-2, Toll-6* and *kek-6*. Altering the levels of DNT-2 or Toll-6 could also modify dopamine-dependent behaviours, including locomotion and long-term memory. We conclude that an activity-dependent feedback loop involving dopamine and DNT-2 labelled the circuits engaged, and DNT-2 with Toll-6 and Kek-6 induced structural plasticity in this circuit, modifying brain function.

SHORT BLURB

Drosophila neurogenetics reveals a novel mechanism of neural circuit structural plasticity, providing insights into how experience modifies brain structure and resulting memory and behaviour.

INTRODUCTION

The brain can change throughout life, as new cells are formed or eliminated, axonal and dendritic arbours grow or shrink, synapses form or are eliminated. Such changes can be driven by experience, that is, neuronal activity or the lack of it [1-9]. Structural changes result in remodelling of connectivity patterns, and these bring about modifications of behaviour. These can be adaptive, dysfunctional or simply reflect opportunistic connections between neurons [10-12]. Importantly, generative structural brain plasticity (e.g. adult neurogenesis, neuronal survival, neurite growth and synaptogenesis) correlates with anti-depressant treatment, learning, physical exercise and well-being [3, 4, 9, 13]. Conversely, structural homeostasis (e.g. cell quiescence, neurite and arbour retraction, synapse elimination) constrains structural change within boundaries that enable appropriate behaviour. However, degenerative processes shared with structural homeostasis also drive neurite, synapse and cell loss, which correlate with ageing, neuroinflammation, psychiatric and neurodegenerative conditions [6, 14-18]. Understanding how experience drives the switch between generative and destructive processes shaping the brain will help us understand brain function, in health and disease. This requires the ability to link with cellular resolution neural circuits, molecular mechanisms and resulting behaviours.

In the mammalian brain, the neurotrophins (NTs: BDNF, NGF, NT3, NT4) are growth factors underlying structural brain plasticity [19-21]. They promote neuronal survival, connectivity, neurite growth, synaptogenesis, synaptic plasticity and Long-Term Potentiation (LTP), via their Trk and $p75^{NTR}$ receptors [19-21]. In fact, all anti-depressants function by stimulating production of BDNF and signalling via its receptor TrkB, leading to increased brain plasticity [13, 22]. Importantly, NTs have dual functions and can also promote structural homeostasis, via $p75^{NTR}$ and Sortilin, to induce neuronal apoptosis, neurite loss, synapse retraction and Long-Term Depression (LTD) [20]. Remarkably, these latter functions are shared with neuroinflammation, which in mammals involves Toll-Like Receptors (TLRs) [23]. TLRs and Tolls across the animals have universal functions in innate immunity [24], and consistently with this, TLRs in the CNS are mostly studied in microglia. However, mammalian *TLRs* are expressed in all CNS cell types, where they can promote not only neuroinflammation, but also neurogenesis, neurite growth and synaptogenesis –

independently of pathogens, cellular damage or disease [25-30]. Whether TLRs have functions in structural brain plasticity and behaviour remains little explored, and whether they can function together with neurotrophins in the mammalian brain is unknown. Furthermore, progress linking cellular events to circuit and behavioural modification has been rather daunting and slow using mammals [16].

Drosophila can expedite discovery. The *Drosophila* adult brain is plastic and can be modified by experience and neuronal activity [31-40]. Different living conditions, simulation with odorants or light, circadian rhythms, long-term memory and experimentally activating or silencing neurons, modify brain volume, alter circuit and neuronal shape, and remodel synapses, revealing both experience-dependent structural plasticity and homeostasis [34-36, 39, 41-46]. Furthermore, the *Drosophila* brain is also susceptible to neurodegeneration [47]. However, the molecular and circuit mechanisms underlying structural brain plasticity and homeostasis are mostly unknown in *Drosophila*.

Toll receptors are expressed across the Drosophila brain, in distinct but overlapping patterns that mark the anatomical brain domains [48]. Tolls share a common transcriptional signalling pathway downstream, that can drive at least four distinct cellular outcomes – cell death, survival, quiescence, proliferation – depending on context [48-50]. They are also required for connectivity and structural synaptic plasticity and they can also induce cellular events independently of signalling [48, 50-56]. Their distribution patterns in the brain and their ability to switch between cellular outcomes means they are ideally placed to translate experience into structural brain change [48].

We had previously observed that in the adult brain, *Toll-6* is expressed in dopaminergic neurons [51]. Dopamine is a key neuromodulator required for both experience and behaviour. It regulates wakefulness and motivation, experience valence, such as reward, and it is essential for locomotion, learning and memory [57-61]. In Drosophila, Dopaminergic neurons (DANs) form an associative neural circuit together with mushroom body Kenyon cells (KCs), Dorsal Anterior Lateral neurons (DAL) and Mushroom Body Output neurons (MBONs) [59, 62, 63]. Kenyon cells receive input from projection neurons of the sensory systems, they then project through the mushroom body lobes where they are intersected by DANs to regulate MBONs to drive behaviour [59, 62]. DAL neurons are required for long-term memory [63].

This associative circuit involving KCs, DANs, DAL and MBONs is required for learning, long-term memory and goal-oriented behaviour [60, 63-66]. During experience, involving sensory stimulation from the external world and from actions, dopamine assigns a value to otherwise neutral stimuli, labelling the associative neural circuits engaged. Thus, this raises the intriguing possibility that a link of Toll-6 to dopamine could enable it to translate experience into circuit modification to modulate behaviour.

In Drosophila, Toll receptors can function both independently of ligand-binding and by binding Spätzle (Spz) protein family ligands, also known as *Drosophila* neurotrophins (DNTs), that are sequence, structural and functional homologues of the mammalian NTs [50, 51, 67-72]. Like mammalian NTs, DNTs also promote cell survival, connectivity, synaptogenesis and structural synaptic plasticity, and they can also promote cell death, depending on context [50, 51, 72-74]. As well as Tolls, DNTs are also ligands for Kekkon (Kek) receptors, kinase-less homologues of the mammalian NT Trk receptors and are required for structural synaptic plasticity [74]. Importantly, the targets regulated by Tolls and Keks - ERK, NFκB, PI3K, JNK, CaMKII – are shared with those of mammalian NT receptors Trk and $p75^{NTR}$ in mammals, with key roles in structural and functional plasticity across the animals [12, 21, 50, 54, 74].

Here, we asked how DNT-2 and its receptors Toll-6 and Kek-6 are functionally related to dopamine, whether they and neuronal activity – as a proxy for experience - can modify neural circuits, and how structural circuit plasticity modifies dopamine-dependent behaviours.

RESULTS

DNT-2A, Toll-6 and Kek-6 neurons are integrated in a dopaminergic and associative circuit

To allow morphological and functional analyses of *DNT-2* expressing neurons, we generated a *DNT-2Gal4* line using CRISPR/Cas9, and drove expression of the membrane-tethered-GFP *FlyBow1.1* reporter. We identified at least 12 DNT-2+ neurons and we focused on four anterior DNT-2A neurons per hemi-brain (Figure 1A). Using the post-synaptic marker Denmark, DNT-2A dendrites were found at the prow (PRW) and flange (FLA) region, whereas axonal terminals visualised with the pre-synaptic marker synapse defective 1 (Dsyd1-GFP) resided at the superior medial protocerebrum (SMP) (Figure 1B,D). We additionally found

post-synaptic signal at the SMP and pre-synaptic signal at the FLA/PRW (Figure 1D), revealing bidirectional communication at both sites. Using Multi-Colour Flip-Out (MCFO) to label individual cells stochastically [75, 76], single neuron clones revealed variability in the DNT-2A projections across individual flies (Figure 1C), consistently with developmental and activity-dependent structural plasticity in Drosophila [33-37, 48, 77]. We found that DNT-2A neurons are glutamatergic as they express the vesicular glutamate transporter vGlut (Figure 1E, left) and lack markers for other neurotransmitter types (Figure S1). DNT-2A terminals overlapped with those of dopaminergic and DAL neurons (Figure 1F,G), suggesting they could receive inputs from neuromodulatory neurons. In fact, single-cell RNA-seq revealed transcripts encoding the dopamine receptors *Dop1R1, Dop1R2, Dop2R* and/or *DopEcR* in DNT-2+ neurons [78]. Using reporters, we found that Dop2R is present in DNT-2A neurons, but not Dop1R2 (Figure 1E right, Figure S1C). Altogether, these data showed that DNT-2A neurons are excitatory glutamatergic neurons that could receive dopaminergic input both at PRW and SMP.

DNT-2 functions via Toll-6 and Kek-6 receptors, and *Toll-6* is expressed in DANs [51]. To identify the cells expressing *Toll-6* and *kek-6* and explore further their link to the dopaminergic system, we used *Toll-6Gal4 [48]* and *kek-6Gal4* [74] to drive expression of membrane-tethered *FlyBbow1.1* and assessed their expression throughout the brain. Using anti-Tyrosine Hydroxilase (TH) - the enzyme that catalyses the penultimate step in dopamine synthesis - to visualise DANs, we found that Toll-6+ neurons included PAMs, PPL1 and PPL2 (Figure 1H, Figure S2D,F Table S1), whilst Kek-6+ neurons included PAM, PAL, PPL1, PPM2 and PPM3 dopaminergic clusters (Figure 1I, Figure S2B,E,F Table S1). DNT-2 can also bind various Tolls and Keks promiscuously [50, 51] and other *Tolls* are also expressed in the dopaminergic system: PAMs express multiple *Toll* receptors (Figure S2F) and all PPL1s express at least one *Toll* (Figure S2F). Using MCFO clones revealed that both *Toll-6* and *kek-6* are also expressed in Kenyon cells [48] (Figure S2I,J, Table S1), DAL neurons (Figure 1K; Figure S2G,H, Table S1) and MBONs (see also Figure S2A-C and Supplementary Text S1). In summary, *Toll-6* and *kek-6* are expressed in DANs, DAL, Kenyon cells and MBONs. These cells belong to a circuit required for associative learning and long-term memory and behavioural output, and DANs are also required for locomotion [58, 59, 62, 63, 65, 66, 79] .

Altogether, our data showed that DNT-2A neurons are glutamatergic neurons that could receive dopamine as they contacted DANs and expressed the *Dop2R* receptor, and that in turn DANs expressed the DNT-2 receptors *Toll-6* and *kek-6*, and therefore could respond to DNT-2. These data suggested that there is bidirectional connectivity between DNT-2A neurons and DANs, which we explored below.

Bidirectional connectivity between DNT-2A neurons and DANs

To verify the connectivity of DNT-2A neurons with DANs, we used various genetic tools. To identify DNT-2A output neurons, we used TransTango [80] (Figure 2A and Figure S3). DNT-2A RFP+ outputs included a subset of MB $\alpha'\beta'$ lobes, $\alpha\beta$ Kenyon cells, tip of MB $\beta'2$, DAL neurons and dorsal fan-shaped body layer and possibly PAM or other dopaminergic neurons (Figure 2A, see Figure S3). Consistently, these DNT-2A output neurons express *Toll-6* and *kek-6* (Supplementary Table S1). To identify DNT-2A input neurons, we used BAcTrace [81]. This identified PAM DAN neuron inputs at SMP (Figure 2B). Altogether, these data showed that DNT-2A neurons receive dopaminergic neuro-modulatory inputs, their outputs include MB Kenyon cells and DAL neurons, and DNT-2 arborisations at SMP are bidirectional.

To further test the relationship between DNT-2A neurons and DANs, we first asked whether activating DNT-2A neurons could induce calcium signalling in PAMs. We activated DNT-2 neurons with optogenetics (CsChrimson) and visualised GCaMP6 fluorescence intensity in PAMs, in live imaging experiments. This revealed a calcium increase in PAMs upon DNT-2-neuron activation (Figure 2C), confirming that DNT-2A neurons are functionally connected to PAMs. Next, we reasoned that stimulating DANs would provoke either release or production of dopamine. So we asked whether increasing DNT-2 levels in DNT-2 neurons could influence dopamine levels. For this, it was necessary to over-express *DNT-2* in full-length form (i.e. *DNT-2FL*), as it enables to investigate non-autonomous functions of DNT-2 [74]. Importantly, DNT-2FL is spontaneously cleaved to the mature form [50, 82] (see discussion). Thus, we over-expressed *DNT-2FL* in DNT-2 neurons and asked whether this affected dopamine production. We were not able to measure changes in dopamine, so we measured mRNA levels for *TH* instead. Using quantitative real-time PCR (qRT-PCR), we found that over-expressing *DNT2-FL* in DNT-2 neurons in adult flies increased

TH mRNA levels in fly heads (Figure 2D). This showed that DNT-2 could stimulate dopamine production in neighbouring DANs.

Next, we wondered whether in turn DNT-2A neurons, that express *Dop2R*, could be modulated by dopamine. Binding of dopamine to D2-like Dop2R (also known as DD2R) inhibits adenylyl-cyclase, decreasing cAMP levels [83, 84]. Thus, we asked whether DNT-2A neurons received dopamine and signal via Dop2R. Genetic restrictions did not allow us to activate PAMs and test DNT-2 neurons, so we activated DNT-2 neurons and tested whether *Dop2R* knock-down would increase cAMP levels. We used the FRET-based cAMP sensor, Epac1-camps-50A [85]. When Epac1-camps-50A binds cAMP, FRET is lost, resulting in decreased YFP/CFP ratio over time. Indeed, *Dop2R* RNAi knock-down in DNT-2A neurons significantly increased cAMP levels (Figure 2E), demonstrating that normally Dop2R inhibits cAMP signalling in DNT-2A cells. Importantly, this result meant that in controls, activating DNT-2A neurons caused dopamine release from DANs that then bound Dop2R to inhibit adenylyl-cyclase in DNT-2A neurons; this inhibition was prevented with *Dop2R* RNAi knock-down. Altogether, this shows that DNT-2 up-regulated TH levels, whereas dopamine inhibited cAMP in DNT-2A neurons (Figure 2F).

In summary, DNT-2A neurons are connected to DANs, DAL and MB Kenyon cells, all of which express DNT-2 receptors *Toll-6* and *kek-6* and belong to a dopaminergic as well as associative learning and memory circuit. Furthermore, DNT-2A and PAM neurons form bidirectional connectivity (Figure 2F): TransTango, EPAC and GCaMP data showed that PAMs are DNT-2 output neurons, and BAcTrace and EPAC data showed that PAMs are DNT-2 input neurons. Finally, DNT-2 and dopamine regulate each other (Figure 2F): DNT-2 increased dopamine levels, and in turn dopamine via Dop2R inhibited cAMP signalling in DNT-2A neurons. That is, an amplification was followed by negative feedback. This suggested that a dysregulation in this feedback loop could have consequences for dopamine-dependent behaviours and for circuit remodelling by the DNT-2 growth factor ligand.

DNT-2 and Toll-6 maintain PAM cell survival in the adult brain

Above we showed that DNT-2 and PAM neurons are connected, so we next asked whether loss of function for *DNT-2* or *Toll-6* would affect PAMs. In wild-type flies, PAM DAN number can vary between 220-250 cells per *Drosophila* brain, making them ideal to investigate changes in cell number [86]. Maintenance of neuronal survival is a manifestation of structural brain plasticity in mammals, where it depends on the activity-dependent release of BDNF [16, 20]. Importantly, cell number can also change in the adult fly, as neuronal activity can induce neurogenesis via Toll-2, whereas DANs are lost in neurodegeneration models [48, 87]. Thus, we asked whether DNT-2 influences PAM number in the adult brain. We used *THGal4; R58E02Gal4* to visualise nuclear Histone-YFP in DANs (Figure 3A) and counted automatically YFP+ PAMs using purposely developed DeadEasy DAN software. $DNT2^{37}/DNT2^{18}$ mutant adult brains had fewer PAMs than controls (Figure 3B). Similarly, *Toll-6* RNAi knock-down in DANs also decreased PAM neuron number (Figure 3C). DAN loss was confirmed with anti-TH antibodies, as there were fewer TH+ PAMs in $DNT2^{37}/DNT2^{18}$ mutants (Figure 3D). Importantly, PAM cell loss was rescued by over-expressing activated $Toll\text{-}6^{CY}$ in DANs in *DNT-2* mutants (Figure 3D). Altogether, these data showed that DNT-2 functions via Toll-6 to maintain PAM neuron survival.

To ask whether DNT-2 could regulate dopaminergic neuron number specifically in the adult brain, we used $tubGal80^{ts}$ to conditionally knock-down gene expression in the adult. PAMs were visualised with either *R58E02LexA>LexAop-nls-tdTomato* or *THGal4; R58E02Gal4 >histone-YFP* and counted automatically. Adult specific *DNT-2* RNAi knock-down decreased Tomato+ PAM cell number (Figure 3E). Similarly, RNAi *Toll-6* knock-down in DANs also decreased PAM neuron number (Figure 3F). Furthermore, knock-down of either *Toll-6* or *DNT-2* in the adult brain caused loss of TH+ PAM neurons (Figure 3G). Cell loss was due to cell death, as adult specific *DNT-2 RNAi* knock-down increased the number of cells labelled with anti-*Drosophila* Cleave caspase-1 (DCP-1) antibodies compared to controls (Figure 3H). This included Dcp-1+ PAMs (Figure 3H). By contrast, *DNT-2FL* over-expression in DNT2 neurons did not alter the incidence of apoptosis, consistently with the fact that DNT-2FL spontaneously cleaves into the mature form [50, 51]. Thus, *DNT-2* and *Toll-6* knock-down specifically in the adult brain induced apoptosis and PAM-neuron loss.

To conclude, these data showed that sustained PAM neuron survival in development and in the adult brain depends on DNT-2 and Toll-6, and a reduction in their levels causes DAN cell loss, characteristic of neurodegeneration.

DNT-2 and its receptors are required for arborisations and synapse formation

We next asked whether DNT-2, Toll-6 and Kek-6 could influence dendritic and axonal arbours and synapses, of neurons within their identified network, that could be analysed with high resolution: PAMs, PPL1 and DAL neurons (Figure 4C). PAM-β2β'2 neurons express *Toll-6* (Table S1), their dendrites overlap axonal DNT2 projections and can be imaged. We first tested the effect of constant knock-down or over-expression from development to adult. *Toll-6* RNAi knock-down in PAM -β2β'2 (with split-GAL4 *MB301BGal4*), reduced dendrite complexity (Figure 4A). To test whether DNT-2 could alter these dendrites, we over-expressed mature *DNT-2CK*. DNT-2CK is not secreted from transfected S2 cells, but it is functional in vivo [50, 72, 74]. Importantly, over-expressed *DNT-2CK* functions cell-autonomously whereas *DNT-2FL* functions also non-autonomously, but they have similar effects [50, 72, 74]. Over-expression of *DNT-2CK* in PAM -β2β'2 increased dendrite arbour complexity (Figure 4B). Thus, during development, DNT-2 and its receptor Toll-6 are required for dendrite growth and complexity in PAM neurons.

To ask whether DNT-2 could affect axonal terminals, we tested PPL1 axons. PPL1-γ1-pedc neurons have a key function in long-term memory [65, 88-90], and express both *Toll-6* and *kek-6* (Table S1). Using split-GAL4 line M*B320C-Gal4* to visualise PPL1 axonal arbours, RNAi knock-down of either *Toll-6*, *kek-6* or both together caused axonal misrouting away from the mushroom body peduncle (Figure 4D,D', Chi Square $p<0.05$, see Table S2). Similarly, *DNT-2FL* over-expression also caused PPL1 misrouting (Figure 4E, Chi-Square $p<0.05$, see Table S2). Thus, during development, DNT-2, Toll-6 and Kek-6 are required for appropriate targeting and connectivity of PPL1 DAN axons.

DAL neurons were identified as outputs of DNT-2 neurons expressing *kek-6* and *Toll-6* (Figure 1K, Figure 2A, Figure S2G,H, Table S1). DAL neurons arborise in SMP, superior lateral protocerebrum (SLP) and anterior optic tubercle (AOTU) [63]. To visualise DAL dendritic arbours and synapses, we expressed the

tagged post-synaptic density (PSD) marker *Homer-GCaMP* (hereby also called *Homer-GFP)* [91], and focused on DAL-SLP arborisations as they can be imaged with single cell, single arbour resolution (Figure 4F-H). We first asked whether DAL dendrites might be affected during development in *DNT-2* mutants, and they were. *DNT-2*^{37}/*DNT-2*^{18} mutants had smaller and simpler DAL dendrites, with fewer synapses and reduced synaptic density (PSD/total dendrite length) (Figure 4F). These data showed that DNT-2 is required in development for DAL dendrite growth and synapse formation. PSD volume increased, perhaps revealing a compensatory response to decreased synapse number (Figure 4F). In fact, increased PSD size in response to decreased activity is a manifestation of homeostatic plasticity also in mammals [18].

Next, we asked whether DNT-2 and Toll-6 were also required in the adult brain. Using *tubGAL80*^{ts}, we over-expressed untagged *DNT-2CK* or *DNT-2FL* in DAL neurons in the adult brain, and this caused an increase in DAL dendrite branching (Figure 4G). Homer-GFP+ synapse density was unaltered (Figure 4G), but as dendritic complexity increased, this suggests synaptic remodelling took place. In fact, PSD volume decreased (Figure 4G), suggesting either that DNT-2 caused a decrease in PSD size, or that this was a compensatory homeostatic adjustment to raised function. By contrast, adult-specific RNAi knock-down of *Toll-6*, *kek-6* or both did not affect DAL-SLP dendritic complexity, but it decreased synapse number and synapse density and caused a compensatory increase in PSD size (Figure 4H). *DNT-2* mutants had a more severe phenotype in dendrite morphology than adult *Toll-6 kek-6* RNAi knock-down, perhaps because RNAi knock-down is not as effective as null mutations, or perhaps revealing a function for DNT-2 throughout dendrite development, or perhaps suggesting that DNT-2 could also function with other Toll and Kek receptors, as it can also bind at least Toll-7 and Kek-5 [51, 74]. In any case, these data showed that DNT-2, Toll-6 and Kek-6 are required for dendrite branching, synapse formation and/or stability in DAL neurons of the adult brain.

To conclude, these data showed that DNT-2, Toll-6 and Kek-6 are required for dendrite branching, axonal targeting and synapse formation in development and in the adult brain. The shared phenotypes from altering the levels of *DNT-2* and *Toll-6 kek-6* in arborisations and synapse formation, support their

joint function in these contexts. Importantly, these findings showed that connectivity of PAM, PPL1 and DAL neurons depend on DNT-2, Toll-6 and Kek-6.

Activity-dependent synaptic remodelling in DAL dendrites requires DNT-2, Toll-6 and Kek-6

The above data showed that DNT-2, Toll-6 and Kek-6 are required for arborisations and synapse formation or stabilisation in development and in adults. Thus, we wondered whether they could also be involved in activity-dependent structural plasticity or homeostasis. We asked whether neuronal activity might affect arborisations of DNT-2 target neurons, and initially focused on DAL-SLP dendrites because they can be measured with single cell, single arbour resolution. Neuronal activity can induce ghost boutons, immature synapses that are later eliminated [92], but a post-synaptic marker like Homer-GFP can reveal stable and remodelled synapses. Genetic limitations did not allow us to activate DNT-2 neurons and concomitantly visualise post-synaptic sites with Homer-GFP in DAL neurons. So we activated DAL neurons using the cation channel TrpA1, which opens with a temperature rise, and visualised the DAL-SLP dendrite with Homer-GFP. We found that neuronal activity decreased dendrite complexity and size (Figure 5A), but it did not affect synapse number nor size, thus resulting in increased synapse density (PSD/dendrite length, Figure 5A). These phenotypes can be explained by: (1) Activity-dependent dendrite size reduction is a homeostatic response to increased pre-synaptic sites [18, 93]. (2) Neuronal stimulation results in the formation and stabilisation of some synapses and the elimination of others, leading to synaptic remodelling [2, 18, 94]. This suggests that activity induced synaptic remodelling in the DAL dendrite.

Thus, we asked whether DNT-2, Toll-6 and kek-6 are required for activity-dependent structural homeostasis or synaptic remodelling. As we had seen before, $DNT2^{37}/DNT2^{18}$ mutants had simpler DAL dendrites with fewer synapses than wild-type, unstimulated controls (Figure 4F). When DAL neurons were activated in $DNT2^{37}/DNT2^{18}$ mutants, there was a reduction in dendrite complexity, but no difference in dendrite length nor synapse density with (30°C) or without (18°C control) neuronal activity (Figure 5B). Since dendrite complexity was not rescued (Figure 5B), this means that DNT-2 is not required for activity-dependent dendrite contraction (i.e. structural homeostasis), and instead is consistent with DNT-2 being

required for dendrite growth. However, the activity-dependent increase in synapse density did not occur in *DNT2*^{37}/*DNT2*^{18} mutants (Figure 5B), meaning that DNT-2 is required for activity-dependent synapse formation. PSD volume increased in *DNT2*^{37}/*DNT2*^{18} mutants upon activation (Figure 5B), consistently with this being a compensatory response that does not require DNT-2, in a context of synapse loss. Altogether, these data showed that activity-dependent dendrite contraction does not require DNT-2, but synapse remodelling does.

Similarly, adult-specific *Toll-6 kek-6* RNAi knockdown did not rescue the effect of activity in dendrite size or complexity either (Figure 5C), meaning that Toll-6 and Kek-6 are not required for activity-dependent dendrite structural homeostasis. By contrast, *Toll-6 kek-6* RNAi knockdown prevented activity-induced synapse remodelling, as synapse number and synapse density both decreased upon activation (Figure 5C). Altogether, these data showed that, like in development, activity-induced synaptic formation depends on Toll-6 and Kek-6, as well as DNT-2.

To conclude, neuronal activity induced structural homeostasis (i.e. decreased dendrite size and complexity) and structural synaptic plasticity (i.e. increased synapse formation and remodelling) in DAL neurons. Structural homeostasis of DAL neurons did not require DNT-2, Toll-6 or Kek-6, consistently with their requirement for dendrite growth instead. On the other hand, activity-induced structural synaptic plasticity depends on DNT-2 and its receptors Toll-6 and Kek-6.

DNT-2 neuron activation and *DNT-2* over-expression induced synapse formation in PAM target neurons

Data above were consistent with DNT-2 promoting synapse remodelling. It was important to explore this further, as in mammals, neuronal activity induces translation, release and cleavage of BDNF, and BDNF drives synaptogenesis [16, 17, 19, 20]. Thus, we first asked whether neuronal activity could influence DNT-2 levels or function. We visualised tagged DNT-2FL-GFP in adult brains, activated DNT-2 neurons with TrpA1 at 30°C, and found that DNT-2 neuron activation increased the number of DNT-2-GFP vesicles produced (Supplementary Figure S5A). Furthermore, neuronal activity also facilitated cleavage of DNT-2 into its mature form. In western blots from brains over-expressing *DNT-2FL-GFP*, the levels of full-length DNT-2FL-

GFP were reduced following neuronal activation and the cleaved DNT-2CK-GFP form was most abundant (Supplementary Figure S5B). These findings were consistent with DNT-2 having activity-dependent functions.

Thus, we asked whether neuronal activity and DNT-2 could increase synapse formation. Bearing in mind that distinct neuron types could elicit distinct responses, we first tested DNT-2 neurons. Activating DNT-2 neurons altered DNT-2 axonal arbours (Figure 6A) and it increased Homer-GFP+ synapse number in the DNT-2 SMP arbour (Figure 6B). Next, as DNT-2 and PAMs form bidirectional connexions at SMP (Figure 1, 2), we asked whether activating DNT-2 neurons could affect target PAM neurons. To manipulate DNT-2 neurons and visualise PAM neurons concomitantly, we combined *DNT-2GAL4* with the *PAM-LexAOP* driver. However, there were no available *LexA/OP* post-synaptic reporters, so we used the pre-synaptic *LexAOP-Syt-GCaM*P reporter instead, which labels Synaptotagmin (Syt) and can be visualised with GFP antibodies. With this tool it was not possible to trace PAM arbours, but we could analyse synapses. Activating DNT-2 neurons with TrpA1 increased the number of Syt+ synapses at the PAM SMP arbour (Figure 6C) and reduced their size (Figure 6C). This was consistent with the increase in Homer-GFP+ PSD number in stimulated DNT-2 neurons (Figure 6B), suggesting newly formed synapses were stable. PAM neurons also send an arborisation at the MB lobes, but DNT-2 neuron activation did not affect synapse number nor size there (Figure 6C). These data showed that activating DNT-2 neurons induced synapse formation at the SMP connection with PAMs.

Finally, we asked whether, like activity, DNT-2FL could also drive synaptogenesis. We over-expressed *DNT-2FL* in DNT-2 neurons and visualised the effect in PAM neurons. Over-expression of *DNT-2FL* in DNT-2 neurons did not alter Syt+ synapse number at the PAM SMP dendrite, but it increased bouton size (Figure 6D). By contrast, at the MB lobe arborisation, over-expressed *DNT-2* did not affect Syt+ bouton size, but it increased the number of output synapses (Figure 6D). This data showed that DNT-2 released from DNT-2 neurons could induce synapse formation in PAM target neurons.

Altogether, these data showed that neuronal activity induced synapse formation, it stimulated production and cleavage of DNT-2, and DNT-2 could induce synapse formation in target neurons.

Structural plasticity by DNT2 modified dopamine-dependent behaviour

Circuit structural plasticity raises the important question of what effect it could have on brain function, i.e. behaviour. Data above showed that DANs and DNT-2 neurons are functionally connected, that loss of function for *DNT-2* or its receptors caused dopaminergic neuron loss, altered DAN arborisations and caused synapse loss, and that DNT-2 could induce dendrite branching and synaptogenesis, altogether modifying circuit connectivity. Next, to measure the effect of such circuit modifications on brain function, we used dopamine-dependent behaviours as readout.

Startle-induced negative geotaxis (also known as the climbing assay) is commonly used as a measure of locomotor ability and requires dopamine and specifically PAM neuron function [95, 96]. We tested the effect of *DNT-2* or *Toll-6* and *kek-6* loss of function in climbing, and both *DNT-2*^{37}/*DNT-2*^{18} mutants and flies in which *DNT-2* was knocked-down in DNT-2 neurons in the adult stage had lower climbing ability than controls (Figure 7A). Similarly, when *Toll-6* and *kek-6* were knocked-down with RNAi in the adult using a Toll-6 or a PAM neuron driver, climbing was also reduced (Figure 7B). Importantly, over-expressing activated *Toll-6*^{CY} in DANs rescued the locomotion deficits of *DNT-2* mutants, showing that DNT-2 functions via Toll-6 in this context (Figure 7C).

We also tracked freely moving flies in an open arena [97]. Interestingly, in that setting, locomotion of homozygous *DNT-2*^{37}/*DNT-2*^{18} mutants was similar to that of controls, but over-expression of *Toll-6*^{CY} in their DANs increased locomotion as flies walked longer distances and spent less time immobile (Figure 7D). Adult flies over-expressing *DNT2-FL* walked faster (Figure 7E and Figure S6) and so did those where DNT-2 neurons were activated with TrpA1 (Figure 7F and Figure S6), consistently with the fact that neuronal activity increased DNT-2 production (Figure S4A) and that DNT-2FL increased TH levels (Figure 2D). Therefore, increased Toll-6^{CY} levels in DANs increase locomotion and increased DNT-2 levels are sufficient to boost walking speed. Interestingly, both loss and gain of function for *DNT-2* also caused seizures (Figure S7). Thus, dopamine-dependent locomotion is regulated by the function of DNT-2, Toll-6 and Kek-6.

Next, as dopamine is an essential neurotransmitter for learning and memory [58, 59], we asked whether DNT-2 might influence appetitive olfactory conditioning. Starved flies were trained to associate a sugar reward with an odour (CS+) while another odour was presented without sugar (CS-), and their preference for CS+ versus CS- was measured, 24h after training (as in [64, 98]). Remarkably, over-expression of *DNT-2FL* in DNT-2 neurons in adults enhanced appetitive long-term memory (Figure 7G), consistent with the positive role of DNT-2 in synaptogenesis that we demonstrated above. We further hypothesised that activating DNT-2 neurons with TrpA1 during memory consolidation could have a positive effect on memory performance through increased DNT-2 production and cleavage and the resulting facilitation of synaptic remodelling. To test this, we artificially activated DNT-2 neurons for 6 hours immediately after training, however memory performance in these flies was only significantly different to one, but not both controls (Supplementary Figure S8, right). Therefore, unlike *DNT-2* overexpression, activation of DNT-2 neurons during consolidation is not sufficient to increase memory performance. Nevertheless, our results show that DNT-2 can enhance appetitive long-term memory.

In summary, using dopamine-dependent locomotion and long-term memory as behavioural readouts, we have shown that alterations in DNT-2, Toll-6 and Kek-6 levels that caused structural phenotypes in PAMs, PPL1 and DAL neurons also modified behaviour.

DISCUSSION

We provide a novel molecular mechanism of structural brain plasticity, identify a neural circuit involved and show how structural modification of this circuit modifies behaviour. Dopamine is a neuromodulator that assigns experience valence and modulates behaviour. The neurotrophin DNT-2 and its receptors Toll-6 and the kinase-less Trk family Kek-6 are linked to the neural circuit involving dopaminergic and DAL neurons. DNT-2 sculpts these circuits in development, in the adult brain and with neuronal activity, by promoting neuronal survival, axon targeting, dendrite branching and synaptogenesis. Our findings suggest that upon neuronal stimulation, dopamine labels the neural circuits engaged and the DNT-2 growth factor sculpts

these circuits, to enhance locomotion and long-term memory. These findings suggest that DNT-2 is a plasticity factor that could enable experience-dependent behavioural adaptation in *Drosophila.*

A closed loop between experience and behaviour could drive brain plasticity vs. degeneration

Our findings support the view that structural plastic and degenerative processes in the brain are two manifestations of a shared underlying molecular mechanism that can be modulated by experience [16, 48]. DNT-2 induced structural plasticity, as it maintained cell survival, induced dendritic complexity and synaptogenesis. Furthermore, neuronal activity up-regulated DNT-2 levels, triggered DNT-2 cleavage, and induced synaptic remodelling, which depended on DNT-2, Toll-6 and Kek-6, and increased DNT-2 levels induced synaptogenesis and enhanced locomotion and long-term memory. Conversely, loss of function for *DNT-2*, *Toll-6* and *kek-6* induced apoptosis, dopaminergic neuron loss, decreased dendritic complexity, impaired targeting, caused synapse loss and impaired locomotion. These phenotypes support previous findings that Toll-6 can promote cell survival and connectivity in development [50][3] and that together with Kek-6 it promotes synaptogenesis at the larval NMJ [74]. Similarly, Toll-2 is also neuro-protective in the adult fly brain, and loss of *Toll-2* function caused neurodegeneration and impaired behaviour [48]. Our findings mean that the levels of DNT-2 could determine whether the brain responds in a plastic and generative manner to experience. This is reminiscent of the link between BDNF deficits and brain disease in humans, and the BDNF-dependent plasticity inducing function of anti-depressants [16, 17, 22].

Neuronal activity caused dendritic arbour retraction, synapse remodelling in DAL neurons and synapse formation in PAM neurons. This is consistent with structural dendrite homeostasis, whereby activity induces dendrite contraction to regulate homeostatically the increase in pre-synaptic sites to modulate input [18, 93]. Synaptic remodelling is the concerted gain and loss of synapses as a consequence of concurring forms of activity-dependent plasticity and leads to modification in connectivity patterns [18, 94]. Our data showed that, in the context analysed, *DNT-2, Toll-6* and *kek-6* were not required for activity-dependent dendrite structural homeostasis, but instead were required for and could drive dendrite branching and synapse formation. This is consistent with their functions promoting axonal arbour growth,

branching and synaptogenesis at the NMJ [74]. It also suggests that other mechanisms regulate structural dendrite homeostasis, which could still include other Spz family ligands, Tolls and Keks. There are six *spz*, nine *Toll* and six *kek* genes in *Drosophila* [74, 99-101], and at least seven *Tolls* and three adaptors are expressed in distinct but overlapping patterns in the brain [48]. Different Tolls could be distributed in different neuronal types or sub-cellular locations (e.g. dendrites vs. axons), different neurons could have distinct intracellular adaptors and could drive distinct cellular outcomes. The combinatorial complexity of DNTs, Tolls and Keks opens the possibility for a fine-tuned regulation of structural circuit plasticity and homeostasis in the brain.

Neuronal stimulation of DNT-2 neurons induced synapse formation in PAM neuron SMP dendrites, whereas DNT-2 over-expression from DNT-2 neurons increased synapse size at the SMP dendrite and induced synaptogenesis in PAM outputs at the mushroom body lobes. Our current data do not fully explain these distinct effects, but they could reflect the range of action. Neuronal activity can induce localised protein synthesis that facilitates local synaptogenesis and stabilises emerging synapses [18]. By contrast, DNT-2 is a growth factor that requires signal transduction to reach the nucleus, and this in turn can facilitate synaptogenesis at longer distances, in output sites. On the other hand, over-expressed DNT-2 is likely to be present in higher levels than activity-dependent DNT-2 production, potentially resulting in homeostatic switch off at the SMP site, consistently with the compensatory increase in PSD size at this location.

It was remarkable to find that dopaminergic neurons in the *Drosophila* adult brain require sustained trophic support, and this is functionally relevant as it can influence behaviour. Loss-of function for *DNT-2, Toll-6* and *kek-6* caused DAN apoptosis and loss and it impaired locomotion. Like in humans, Dopamine is required for locomotion in *Drosophila*, and specifically in PAMs for climbing [57, 95, 96]. Importantly, *Drosophila* models of Parkinson's Disease reproduce the loss of DANs and locomotion impairment found in human patients [57, 87, 95, 96]. Conversely, *DNT-2* gain of function and neuronal activation of DNT-2 neurons enhanced locomotion, consistently with the fact that neuronal activity increased DNT-2 levels, and DNT-2 upregulated *TH* expression. These data show that the adult Drosophila

brain is not static, but instead cells receive secreted growth factors that maintain brain integrity, and structural brain change impacts behaviour.

We showed that the structural circuit modifications by DNT-2 with Toll-6 and Kek-6 modulated dopamine-dependent behaviours, including as well as locomotion, also long-term memory. Dopamine is also required for associative reward learning and long-term memory [58, 59]. In Drosophila, this requires PAM, PPL1 and DAL neurons and their connections to Kenyon Cells and MBONs [59, 62, 63, 66]. We showed that DNT-2 neurons are connected to all these neuron types, which also express *Toll-6* and *kek-6*; that altering the levels of DNT-2, Toll-6 and kek-6 affected arborisations and synaptogenesis in DAL and DANs, and behaviour; that neuronal activity remodelled DAL synapses, and this required *DNT2, Toll-6* and *kek-6*; and that over-expression of *DNT-2* increased TH levels, DAL dendrite complexity, induced synaptogenesis in PAM neurons and enhanced locomotion and long-term memory. Altogether, these data demonstrate that structural circuit changes caused by altering the levels of DNT-2, Toll-6 and Kek-6 modified dopamine-dependent behaviours, providing a direct link between structural brain change and behavioural modification. We used neuronal activation as a proxy for experience, but the implication is that experience would similarly drive the structural modification of circuits labelled by neuromodulators. Since behaviour is a source of experience, this provides a mechanistic basis for closed loops between experience and behaviour that shape the brain throughout life.

Deep evolutionary roots, novel branches?

It is important to identify the molecules responsible for shaping the brain and our work has shown that this can be done using Drosophila as a model organism.

There is deep evolutionary conservation in DNT-2 vs mammalian NT function (eg BDNF), with some peculiarities too. Like mammalian NTs, full-length DNTs/Spz proteins contain a signal peptide, an unstructured pro-domain and an evolutionarily conserved cystine-knot of the neurotrophin family [50, 72, 102]. Cleavage of the pro-domain releases the mature cystine-knot (CK). In mammals, full-length neurotrophins have opposite functions to their cleaved forms (e.g. apoptosis vs cell survival, respectively).

However, this is not the case for DNT-2. DNT-2FL is cleaved spontaneously by intracellular furins, and although DNT-2 can be found both in full-length or cleaved forms in vivo, it is most abundantly found cleaved [50, 51, 72]. As a result, over-expressed *DNT-2FL* does not induce apoptosis and instead it promotes cell survival [50]. The same functions are played by over-expressed mature *DNT-2-cystine knot* (*DNT-2CK*) as by *DNT-2FL* [50, 72, 74]. In S2 cells, transfected DNT-2CK is not secreted, but when over-expressed in vivo it is functional [50, 72, 74] (and this work). In fact, over-expressed *DNT-2CK* also maintains neuronal survival, connectivity and synaptogenesis [50, 72, 74] (and this work). Similarly, over-expressed mature *spz-1-C106* can rescue the *spz-1*-null mutant phenotype [103] and over-expressed *DNT-1CK* can promote neuronal survival, connectivity and rescue the *DNT-1* mutant phenotype [72]. Consistently, both DNT-2FL and DNT-2CK have neuro-protective functions promoting cell survival, neurite growth and synaptogenesis [50, 72-74] (and this work). Importantly, over-expressing *DNT-2FL* enables to investigate non-autonomous functions of DNT-2 [74].

We have shown that over-expressed *DNT-2FL* can induce dendrite branching and synaptogenesis, including non-autonomously in target neurons. Similarly, DNT-2 is a retrograde factor at the larval NMJ, where transcripts are located post-synaptically, DNT-2FL-GFP is taken up from muscle by motorneurons and DNT-2FL induced synaptogenesis [73, 74]. Importantly, neuronal activity increased production of tagged DNT-2-GFP, its cleavage and plasticity of DNT-2 neuronal arbours in the brain. In mammals, neuronal activity induces synthesis, release and cleavage of BDNF, leading to neuronal survival, dendrite growth and branching, synaptogenesis and synaptic plasticity (ie LTP) [16, 19, 20, 104, 105]. Like BDNF, DNT-2 also induced synaptogenesis and could increase bouton size, but in other instances caused a decrease in PSD size. It was not always possible to disentangle primary from compensatory phenotypes, as Hebbian, homeostatic and heterosynaptic plasticity concur [18, 94]. Mammalian BDNF has a well-documented function increasing both synapse number, spine size and long-term potentiation (LTP), but it is also involved in homeostatic plasticity and long-term depression (LTD), depending on timing, levels and site of action [16, 19, 20]. On the other hand, although spines can be present in Drosophila [106], the structural repertoire of post-synaptic sites and spines across flies and mammals could have diversified, explaining

distinct responses. Altogether, our findings reveal an evolutionary conserved function of DNT-2 in promoting dendritic complexity and synaptogenesis.

Long-term memory requires synaptogenesis, and in mammals this depends on BDNF [16, 19, 107]. It plays a critical role in the protein-synthesis dependent phase of LTP [16, 19, 107]. BDNF localised translation, expression and release are induced during memory consolidation to enable long-term memory [16, 19, 107, 108]. We have shown that similarly, over-expressed *DNT-2FL* increased long-term memory. Furthermore, tantalising data suggest that *DNT-2* could perhaps also function in the consolidation phase, something to explore further in the future. Altogether, the functions of BDNF and DNT-2 in long-term memory are also conserved.

We have shown that DNT-2 and DAN neurons form bidirectional connectivity that modulates both DNT-2 and dopamine levels. Similarly, mammalian NTs also promote dopamine release and the expression of DA receptors [109, 110]. Importantly, we showed that DAN cell survival is maintained by DNT-2 in *Drosophila.* Similarly, DAN cell survival is also maintained by NT signalling in mammals and fish [111, 112]. We showed that activating DNT-2 neurons increased the levels and cleavage of DNT-2, and up-regulated DNT-2 increased *TH* expression. This initial amplification in turn resulted in the inhibition of cAMP signalling by dopamine via Dop2R in DNT-2 neurons. This negative feedback could drive a homeostatic reset of both DNT-2 and dopamine levels, that could be important for normal brain function. In fact, alterations in both NTs and dopamine underlie many psychiatric disorders and neurodegenerative diseases in humans [16, 18, 110, 112, 113].

This work has uncovered a novel mechanism of structural brain plasticity, involving a NT ligand functioning via a Toll and a kinase-less Trk-family receptor in the adult *Drosophila* brain. Toll receptors in the CNS can function via ligand dependent and ligand-independent mechanisms [49]. However, we showed that in the context analysed, the function of Toll-6 and Kek-6 in structural circuit plasticity depends on DNT-2. In the course of evolution *Drosophila* and mammalian NTs may have evolved to use different receptor types to elicit equivalent cellular outcomes, or further functions of known receptors remain to be uncovered in humans. In fact, in mammals, NTs function via Trk, $p75^{NTR}$ and Sortilin receptors, to activate

ERK, PI3K, NFκB, JNK and CaMKII [16, 20]. Similarly, DNTs with Tolls and Keks also activate ERK, NFκB, JNK and CaMKII in the Drosophila CNS [49-51, 74]. However, Trks have many isoforms, many of them kinase-less and of unknown function [114, 115]. Kinase-less Trks can function as ligand sinks and dominant negative forms, but they can also function independently of full-length Trks, influencing calcium levels, growth cone extension and dendritic growth and are linked to psychiatric disorders, e.g. depression [116-123]. Like Keks, perhaps kinase-less Trks have also evolutionarily conserved functions that can influence brain plasticity vs. degeneration. A functional relationship between NTs and TLRs could exist also in humans, as in cell culture, human neurotrophins BDNF and NGF can induce signalling from a TLR [50]. Importantly, TLRs can regulate cell survival, death and proliferation, neurogenesis, neurite growth and collapse, learning and memory [27]. They are linked to neuroinflammation, psychiatric disorders, neurodegenerative diseases and stroke [27, 124, 125]. Intriguingly, genome-wide association studies (GWAS) have revealed the involvement of TLRs in various brain conditions and potential links between neurotrophins and TLRs in, for example, major depression [126-129]. Importantly, alterations in NT function underlie psychiatric, neurologic and neurodegenerative brain diseases [12, 14, 16, 17, 20-22, 130, 131]. It is compelling to find out whether and how these important protein families interact in the human brain.

Conclusion

To conclude, we have shown that neuronal activity results in an initial amplification of both DNT-2 and TH levels, which regulate each other homeostatically. Dopamine labels the circuits engaged and DNT-2, a growth factor, with its receptors Toll-6 and Kek-6, drives structural plasticity in these circuits, enhancing dopamine-dependent behaviour, including locomotion and memory. Conversely, loss of function for *DNT-2, Toll-6* and *kek-6* causes degeneration and impairs behaviour. Our data provide a direct link between activity-dependent structural modification and the resulting behaviour, by an identified molecular mechanism. An implication is that subjective experience could similarly result in the structural modification of neural circuits labelled by neuromodulators, driving behavioural modification. As behaviour is a source of

experience, this has profound implications for understanding brain function and mental health, that can be further explored using *Drosophila.*

ACKNOWLEDGEMENTS

We thank our lab for discussions and Carolina Rezaval and Thomas Riemensperger for comments on the manuscript; Carolina Rezaval for advice and sharing kit for behaviour experiments; Reinhard Wolf, Martin Heisenberg and Scott Waddell for training on learning and memory tests, for sharing kit and designs, helping us get equipped and for advice; Xiufeng Li for help with programming; Karina Piotrowska for help with behaviour experiments; Serge Birman, Ann-Shyn Chiang, Ron Davis, André Fialá, Barret Pfeiffer, Xi Rao, Carolina Rezaval, Iris Salecker for flies; DSHB (Iowa) for antibodies; AddGene for plasmids; Bloomington Stock Centre for *Drosophila* stocks. This work was funded by Marie-Curie Sklodowska Post-Doctoral fellowship to J.S.; Science Without Borders-CAPES PhD Studentship BEX 13380/13-3 to SUB; BBSRC Project Grants BB/R00871X/1 and BB/P004997/1 to A.H.; and Wellcome Trust Investigator Award 223197/Z/21/Z to A.H.

AUTHOR CONTRIBUTIONS

J.S., V.C designed and executed experiments and analysed data; S.U-B, G.L, D.S, X.W., F.R.C, M.M. executed experiments and analysed data; M.G.F, S.C., A.H. developed tools; D.K., G.J, V.C., A.H. supervised; J.S and A.H. wrote manuscript. A.H. conceived and directed the project, designed experiments, analysed data, wrote manuscript. All authors provided feedback on and contributed to improvements to the manuscript.

DATA AVAILABILITY STATEMENT

All data are contained within the manuscript; metadata and statistical analysis details including full genotypes, sample sizes, statistical tests and p values have been provided in Table S2. This work generated fly stocks and molecular constructs, which we will distribute on request. Raw data will be distributed on request.

DECLARATION OF INTERESTS

The authors declare that they have no conflict of interest.

MATERIALS AND METHODS

Genetics

Mutants: *DNT2*^{37} and *DNT2*^{18} are protein null [50, 74]. *Toll6*^{31} is a null mutant allele [51]. **Driver lines:** *DNT2-Gal4* is a CRISPR/Cas9-knock-in allele, with GAL4 at the start of the gene (this work, see below). *Toll-6-Gal4* was generated by RMCE from *MIMIC Toll-6*^{MIO2127}*; kek6-Gal4* from *MIMIC Kek6*^{MI12953} [48, 74]. *MB320C-Gal4 (BSC68253), MB301B-Gal4 (BSC68311), R58E02-Gal4 (BSC41347), MB247-Gal80 (BSC64306), R58E02-LexA (BSC52740), R14C08-LexA (BSC52473)* were from the *Drosophila* Bloomington Stock Centre (BSC). *Dop1R1-LexA, Dop2R-LexA, Gad-LexA* were kindly provided by Yi Rao; *TH-LexA* (gift of Ron Davis), *TH-Gal4,R58E02-GAL4* (gift of Serge Birman); *G0431-Gal4 (DAL-GAL4), VT49239 nls LexA (DAL LexA)* (gifts from Ann-Shyn Chiang). **Reporter lines:** *UAS-CD8::GFP,* for membrane tethered GFP; *UAS-histone-YFP*, for YFP-tagged nuclear histone; *UASFlybow1.1*, constant membrane tethered expression (gift of Iris Salecker); *13xLexAop-nls-tdTomato,* nuclear Tomato; *UASCD8::RFP, LexAopCD8::GFP* (BSC32229), for dual binary expression; *UAS-homer-GCaMP* for post-synaptic densities (gift of André Fialá),), and *LexAop-Syt-GCaMP* for presynaptic densities (BSC64413). **For connectivity***: UAS-DenMarkRFP, UAS-Dsyd1GFP* (gift of Carolina Rezaval); TransTango: *yw* {*UAS-myrGFP,QUAS-mtdTomato-3xHA}attP8; Trans-Tango@attP40* (BSC77124); BAcTrace 806 *(w;LexAop2-Syb::GFP-P10(VK37) LexAop-QF2::SNAP25::HIVNES::Syntaxin(VK18)/CyO; UAS-B3Recombinase (attP2) UAS<B3Stop<BoNT/A (VK5) UAS<B3Stop<BoNT/A(VK27) QUAS-mtdTomato::HA/TM2*): **MCFO clones**: *hs-FLPG5.PEST;; 10xUAS (FRT.stop) myr::smGdP-OLLAS} 10xUAS (FRT.stop) myr::smGdP-HA 10xUAS (FRT.stop) myr::smGdP-V5-THS-10xUAS (FRT.stop) myr::smGdP-FLAG* (BSC64086). **Live imaging:** cAMP sensor: *UAS-Epac1-camps-50A* (BSC25408); Ca^{2+} sensor: *13XLexAop2-IVS-GCaMP6s-p10 su(Hw)attP1 (BDSC44272), 13XLexAop2-IVS-GCaMP6s-p10 su(Hw) attP5* (BSC44590). **Optogenetic activation:** *20x UAS-V5-Syn-CsChrimson td tomato* (gift of B. Pfeiffer**). For thermogenetic**

activation: *UASTrpA1@attP2 (BSC26264)* and *UAS-TrpA1@attP216 (BSC26263).* **UAS gene over-expression**: *UAS-DNT2CK, UAS-DNT2FL-GFP, UAS-DNT2-FL-47C, UAS-Toll-6^{CY}* [50, 51]. **UAS-RNAi knockdown:** *UAS-DNT2RNAi* (VDRC49195), *UAS-Toll6RNAi* (VDRC928), *y^1v^1; UAS-Toll6RNAi[Trip.HMS04251]* (BSC 56048*), UAS-kek6RNAi* (VDCR 109681), *y^1v^1; UAS-Dop2R-RNAi[TRiP.HMC02988](*BSC50621).

Molecular biology

DNT-2GAL4 was generated by CRISPR/Cas9 enhanced homologous recombination. 1 kb long 5' and 3' homology arms (HA) were amplified by PCR from genomic DNA of wild type flies, using primers for 5'HA: atcgcaccggtttttacaggcaccccatgtctga containing AgeI cutting site and cttgacgcggccgcTGTCAATTCATTCGCCGTCGAT containing NotI cutting site. 3'HA primers were: tattaggcgcgccATGACAAAAAGTATTAAACGTCCGCCC containing AscI cutting site and tactcgactagtgaagcacacccaaaatacccagg containing SpeI cutting site. HAs were sequentially cloned by conventional cloning into pGEM-T2AGal4 vector (Addgene #62894). For gRNA cloning, two 20 nucleotide gRNA oligos (gtcGACAAGTTCTTCTTACCTATG and aaacCATAGGTAAGAAGAACTTGTC) were designed using Optimal Target Finder. BbsI enzyme sites were added: gtc(g) at the 5' end of sense oligo, and aaac at the 5' end of the antisense oligo. gRNA is located at 41 bp downstream of the start codon of DNT-2 within the first coding exon. The gRNA was cloned into pU6.3 using conventional ligation. The two constructs were injected in Cas9 bearing flies and red fluorescent (3xP3-RFP) transformants were selected and balanced, after which 3xP3-RFP was removed with CRE-recombinase.

qRT-PCR

qRT-PCR was carried out from 20 whole adult fruit-fly heads, frozen in liquid nitrogen before homogenising in 50 μl Trizol (Ambion #AM9738), followed by a stand RNA extraction protocol. RNA was treated with DNase treatment (ThermoFisher # AM1906) to remove genomic DNA. 200 ng of RNA was used for cDNA synthesis following Goscript Reverse Transcriptase (Promega #237815) protocol. Sample was diluted 1:4 with Nuclease free H_2O. Standard qPCR was performed with SensiFast syb Green Mix (Bioline #B2092020)

in ABI qPCR plate (GeneFlow #P3-0292) and machine. To amplify TH mRNA the following primers were used: TH-F: CGAGGACGAGATTTTGTTGGC and TH-R: TTGAGGCGGACCACCAAAG. GAPDH was used as a housekeeping control. Reactions were performed in triplicate. Specificity and size of amplification products were assessed by melting curve analyses. Target gene expression relative to reference gene is expressed as value of $2^{-\Delta\Delta Ct}$ (where Ct is the crossing threshold).

Conditional expression

Multiple Colour Flip Out clones: *DNT2-Gal4, Toll6-Gal4* and *kek6-Gal4* were crossed with *hsFLP::PEST;;MCFO* flies, female offspring were collected and heat-shocked at 37°C in a water bath for 15 mins, then kept for 48h at 25°C before dissecting their brains. ***TransTango:*** DNT2-Gal4 or Oregon female virgins were crossed with *TransTango* males, progeny flies were raised at 18°C constantly and 15 days after eclosion, female flies were selected for immunostaining. **Thermogenetic activation with *TrpA1:*** Fruit-flies were bred at 18°C from egg laying to 4 days post-adult eclosion, then shifted to 29°C in a water bath for 24h followed by 24h recovery at room temperature for over-expressed *DNT-2FL-GFP*; for the other experiments, after breeding as above, adult flies were transferred to an incubator at 30°C, kept there for 24h and then brains were dissected. **Conditional gene over-expression and RNAi knockdown:** Flies bearing the temperature sensitive GAL4 repressor tubGal80^{ts} were kept at 18°C from egg laying to adult eclosion, then transferred to 30 °C incubator for 48h for Dcp-1+ and cell counting experiments and for 120h for TH+ cell counting.

Immunostainings

Adult fruit-fly female brains were dissected (in PBS), fixed (in 4% para-formaldehyde, room temperature, 20-30min) and stained following standard protocols. Primary antibodies and their dilutions were as follows: Mouse anti-Brp (nc82) 1:10 (DSHB); Rabbit anti-GFP 1:250 (Thermofisher); Mouse anti-GFP 1:250 (Thermofisher); Chicken anti-GFP 1:500 (Aves); Rabbit anti-FLAG 1:50 (Sigma); Mouse anti-V5 1:50 (Invitrogen); Chicken anti-HA 1:50 (Aves); Rabbit anti-VGlut 1:500 (gift of Hermann); Mouse anti-TH 1:250

(Immunostar); Rabbit anti-TH 1:250 (Novus Biologicals); Rabbit anti-DsRed 1:250 (Clontek); Mouse anti-ChAT4B1 1:250 (DSHB); Rabbit anti-5-HT 1:500 (Immunostar); Rabbit Anti-DCP-1 1:250 (Cell Signalling). Seconday antibodies were all used at 1:500 and all were from Thermofisher: Alexa Flour 488 Goat anti-mouse, Alexa Flour 488 donkey anti-rabbit, Alexa Flour 488 Goat anti-rabbit (Fab')2, Alexa Flour 488 Goat anti-chicken, Alexa Four 546 Goat anti-rabbit, Alexa Four 546 Goat anti-mouse, Alex Four 647 Goat anti-rabbit, Alex Four 647 Goat anti-mouse.

Microscopy and Imaging

Laser scanning confocal microscopy. Stacks of microscopy images were acquired using laser scanning confocal microscopy with either Zeiss LSM710, 900 or Leica SP8. Brains were scanned with a resolution of 1024x1024, with Leica SP8 20x oil objective and 1 μm step for whole brain and DCP-1 stainings, 40x oil objective and 1 μm step for central brain. Resolution of 1024x512 was used for analysing PAM clusters with 0.96 μm step for cell counting; 0.5 μm step for neuronal morphology; and 63x oil objective with 0.5μm step for neuronal connections. Acquisition speed in Leica SP8 was 400Hz, with no line averaging. Resolution of 3072x3072 was used for single image analysis of synapses, using either Leica SP8 or Zeiss LSM900 and Airyscan acquisition with 40x water objective speed 6, and average 4, or with 1024x512, with 40x oil lens 2x zoom and 0.35μm step. TH counting in PAM were scanned with Zeiss 710 with a resolution 1024x1024, 40x oil objective, step 1 μm, speed 8. Zeiss LSM900 Airyscan with a resolution of 1024x1024, 40x water objective, speed 7, 0.7 zoom and 0.31μm step size was used for acquisition of optical sections of synapses in PAM neurons.

Optogenetics and 2-photon microscopy:

1. Real time GCaMP imaging. To ask whether stimulation of DNT-2 neurons could activate output PAM neurons, DNT-2 neurons were depolarised using *DNT-2GAL4>UAS-CsChrimson* and activation of PAM neurons was tested using R58E02LexA driving expression of the LexAopGCaMP6s calcium reporter, *ex vivo*. 1-3 day-old *R58E02LexA DNT2Gal4 UASCsChrimson LexAopGcamp6s* flies were collected and separated into two groups. One group was fed normal food and the second group were fed freshly prepared food

containing 50μM all-trans retinal, vials were wrapped with foil paper in complete darkness, for at least 3 days prior to experiments. Flies were put on ice and brains were dissected in adult hemolymph-like solution (103mM NaCl, 3mM KCl, 5mM N-Tris, 10mM trehalose, 10mM glucose, 7mM sucrose, 26mM $NaHCO_3$, 1mM NaH_2PO_4, 1.5mM $CaCl_2$, 4mM $MgCl_2$). Because of the sensitivity of GCaMP6s, brains were left in the dark for 15-20min after mounting on poly-L-lysine coated slides to prevent any potential brain movements, and subsequently were processed for imaging. The settings for GCaMP6s recording were set according to [132] at a frame rate of 10 Hz, at 925nm using an Olympus FVMPE-RS two-photon microscope with an FV30-FGR filter. To activate CsChrimson optogenetically, each fly was stimulated using a sapphire laser at 588nm, targeting the laser onto DNT-2 projections in the SMP region for 20s. The recording started 10s before the stimulation and lasted 1min after 20s stimulation.

GCaMP image analysis was performed using ImageJ. A region of interest (ROI) was defined where GCaMP intensity was seen to change in response to stimulation. Fluorescence intensity within the ROI was measured across each frame and background fluorescence (F0) was determined as the average of 5 frames before stimulation. Normalised fluorescence intensity dF/F0(GcaMP6s) was calculated for the ROI for each frame after stimulation. Graphs were produced with GraphPad Prism.

2. Epac1 FRET 2-photon imaging. To test whether DNT-2 neurons can respond to dopamine via the Dop2R inhibitory receptor, we used the cAMP sensor Epac1 and 2-photon confocal microscopy. Epac1 is FRET probe, whereby data are acquired from CFP and YFP emission and lower YFP/CFP ratio reveals higher cAMP levels. DNT-2Gal4 flies were crossed to *UAS-CsChrimson UAS Epac1* flies, to stimulate DNT-2 neurons and detect cAMP levels in DNT2 neurons. 1-3 day-old *DNT2Gal4>UASCsChrimson, UAS Epac1* flies were collected and separated in two groups. Flies bearing *DNT2Gal4 UASCsChrimson UAS Epac1 UASDop2RRNAi* were fed on 50μM all-trans retinal food for at least 3 days prior to imaging and kept in constant darkness prior to the experiment.

Optogenetic stimulation of fly brains expressing CsChrimson in DNT-2 neurons was carried out using a sapphire 588nm laser, in a 2-photon confocal microscope. For acquisition of YFP and CFP data from Epac1 samples, a FV30-FYC filter was applied, using a 925nm laser for both YFP and CFP imaging. The

stimulation laser was targeted onto DNT-2 neuron projections in SMP region for 20s. Acquisition ROI was at DNT-2A cell bodies with a frame rate of around 10Hz. The first acquisition started 10s before the 20s stimulation and consequential acquisition was done every 30s for 10 cycles.

Image analysis of Epac data was carried out using ImageJ. The two channels (YFP and CFP) were separated, and the ratio of YFP/CFP for each pixel was calculated using the ImageJ>Image Calculator by diving YFP channel by CFP channel. The obtained result of YFP/CFP ratio was saved and the mean ratio of YFP/CFP in the ROI was calculated for each time point and 11 time points were used. The 11 values represent the ratio of YFP/CFP change in the cell body upon stimulation, with 30s interval and repeated 10 times.

Automatic cell counting with DeadEasy plug-ins: To automatically count cell number labelled with nuclear reporters (e.g. Histone-YFP, nls-tdTomato) and Dcp-1+ cells, we adapted the DeadEasy Central Brain ImageJ plug-in [48]. DeadEasy automatically identifies and counts cells labelled with nuclear reporters in 3D stacks of confocal image in the adult central brain. Brains expressing these reporters were dissected, fixed and scanned without stainings. DeadEasy Central Brain was used with threshold set to 75.

To count the TH labelled PAMs, we purposely developed a newly plug-in called DeadEasy DAN. Since TH-stained images had Poisson noise, a median filter was used to reduce noise, without having large losses at the edges. Then, given that cell walls of irregular intensity are frequently encountered, a 3D morphological closing was performed. Since each cell is identified as a dark area surrounded by pixels of higher intensity and that, in the background, due to noise, it is also possible to find local minima that can be incorrectly identified as cells, all very dark pixels were assigned a value of zero. To mark each cell, each chasm in the image was found using a 3D extended h-minimal transform. As more than one local minimum can be found within each cell, which would result in counting a cell multiple times, a 3D inverse dome detection was performed, and then labelled. Thus, each inverse dome was used as a seed to identify each cell. Once the seeds were obtained, a 3D watershed transformation was performed to recover the shape of the cells. Finally, a colour palette was used to visualize each cell more easily. DeadEasy DAN is accurate in

controls and mutants, but less accurate with RNAi knock-down genotypes, for which it was not used and TH+ cells were counted manually instead, assisted by the ImageJ cell counter.

Dendrite analysis with Imaris: To analyze dendritic complexity, image data were processed with Imaris using the "Filament Autodetect" function with the default algorithm and autopatch function. Setting of the threshold was consistent within the same experiment: the largest or smallest diameter of the dendrite, same threshold for background substation, local contrast. Number of dendritic branches, dendritic segments, dendritic branch points and dendritic terminal points were collected to compare the difference between the groups.

Vesicles, synapses and PSD analysis with Imaris: To analyse the number and volume of Homer-GCaMP GFP+ post-synaptic densities (PSD), Syt-GCaMP GFP+ presynaptic sites and DNT-2FLGFP+ vesicles, optical section images of confocal stacks through the brain were processed with the Imaris Spot function. Setting of the threshold was consistent across experiments.

Brain registration and Nblast: DNT-2 single neurons imaged from *DNT-2GAL4>MCFO* brains were used for brain registration, following the protocol described in [133]. JFRC2 was chosen as the template for DNT-2 neuron registration. Leica SP8 lasering confocal microscopy was used for image acquisition with 20x oil objective, 1024x512, Zoom 0.91 step 1µm, 218 total frames. Fiji with CMTK plug-ins were applied for brain registration. The reformatted brains were opened in Fiji-single neuron trace to obtain the approximate neuron trace of DNT-2 neurons. The obtained neuron traces were uploaded to Nblast to find similar neurons [75].

Behaviour

1. Startle induced negative geotaxis Assay was carried out as described in [96]. Groups of approximately 10 male flies of the same genotype were placed in a fresh tube one night before the test, after which flies were transferred to a column formed with two empty tubes 15cm long and 2cm and then habituated for 30mins. Columns were tapped 3-4 times, flies fell to the bottom and then climbed upwards. Multiple rounds of testing were performed 3-7 times in a row per column. The process was filmed and films were

analysed. Flies were scored during the first 15s after the tapping, and those that climbed above 13cm and those that climbed below 2cm were counted separately. Results given are mean ± SEM of the scores obtained with ten groups of flies per genotype. The performance index (PI) is defined as $1/2[(n_{tot} + n_{top} - n_{bot})/n_{tot}]$, where n_{tot}, n_{top}, and n_{bot} are the total number of flies, the number of flies at the top, and the number of flies at the bottom, respectively. The assay was carried out at 25°C, 55% humidity. Flies with tubGal80^{ts} to conditionally overexpress or knock-down were shifted from 18 to 30°at eclosion and kept for 5 days at 30°C to induce Gal4. Experiments were carried in an environmental chamber at 31°C, 60% humidity or in a humidity and temperature-controlled behaviour lab always kept at 25°C.

2. Spontaneous Locomotion in an open arena: Male flies of each genotype were collected and kept in groups of 10-20 flies, in vials containing fresh fly food for 5-9 days. Before filming, three male flies from one genotype were transferred into a 24 mm well of a multi-well plate using an aspirator and habituated for 15 – 20 mins. The multi-well plate with transparent lid and bottom was placed on a white LED light pad (XIAOSTAR Light Box) and either inside a light-shielding black box (PULUZ, 40*40*40cm) in a room with constant temperature (25°C) and humidity (55%) to maintain stable environmental conditions (Figure 7D), or inside a temperature controlled environmental chamber at 18°C or 30°C (Figure 7E,F,) . The locomotion behaviour of freely-moving flies was filmed with a camera (Panasonic, HC-V260) in the morning from ZT1-ZT4 and for 10 min at a frame-rate of 25 fps. The 10-min videos were trimmed (from 00:02:00 to 00:07:00) to 5-min videos for analysis using Flytracker software (Barwell et al., 2022; Eyjolfsdottir et al., 2014). For the *DNT-2* mutants and over-expression of Toll-6^{CY} experiments, flies were bred and tested at 25 °C. To test over-expression of *DNT-2* with *tubGAL80^{ts}; DNT2-Gal4>UAS-DNT-2FL*, flies were raised at 18°C until eclosion, and controls were kept and tested at 18°C; test groups were transferred directly after eclosion to 30°C for 5 days and were tested in an environmental chamber kept at 30°C, 60%. For thermo-genetic activation of DNT2 neurons using TrpA1 (DNT-2GAL4>UASTrpA1), flies were bred at 18°C and kept at 18°C for 7-9 days post-eclosion. Following habituation at 18°c for 20 mins in the multi-well plates, they were transferred to the 30°C chamber 10 mins before filming to activate TrpA1 and then filmed for the following 10 minutes. Fly locomotion activity was tracked using FlyTracker and calculated (distance and speed) in Matlab [97] using the raw data generated from the tracking

procedure. The “walking distance” was calculated as the sum of the distance flies moved and the “walking speed” was the speed of flies only when they were walking, and it was calculated using only frames where flies moved above 4 mm/s (which corresponds to two body lengths).

3. Appetitive long term memory test: Appetitive long-term memory was tested as described in Krashes and Waddell [98]. The two conditioning odours used were isoamyl acetate, Sigma-Aldrich #24900822, 6µL in 8mL mineral oil (Sigma-Aldrich #330760) and 4-methylcyclohexanol (Sigma-Aldrich # 153095, 10µL in 8mL mineral oil). Groups of 80-120 mixed sex flies were starved in a 1% agar tube filled with a damp 20 x 60 mm piece of filter paper for 18-20 hour before conditioning. During conditioning training, one odorant was presented with a dry filter paper (unconditioned odour, CS-) for 2 minutes, before a 30 second break, and presentation of a second odorant with filter paper coated with dry sucrose (conditioned odour, CS+). The test was repeated pairing the other odorant with sucrose, with a different group of flies to form one replicate. After training, flies were transferred back to agar tubes for testing 24 hours later. Performance index (PI) was calculated in the same way as in Krashes and Waddell [98], as the number of flies approaching the conditioned odour minus the number of flies going in the opposite direction, divided by the total number of flies. A single PI values is the average score from the test with the reverse conditioning odour combination. Groups for which the total number of flies among both odorants was below 15 were discarded. For the *DNT-2* over-expression experiments with *tubGAL80^{ts}; DNT-2>DNT-2FL,* flies were raised at 18°C until 7-9 days post-eclosion. They were then either transferred to and maintained at 23°C (controls) or 30°C for 18-20h starvation, training, and up to testing 24h later. For the thermo-genetic activation of *DNT2-Gal4* with TrpA1 *(DNT-2>TrpA1),* flies were bred at 18°C and kept until 7-9 days old, and either transferred to and maintained at 23°C for the starvation, training and test (controls) or starved at 23°C and moved to 30°C for 6h followed by 23°C for another 18h, until testing after 24h.

Statistical analysis: Statistical analyses were carried out using Graph-Pad Prism. Confidence interval was 95%, setting significance at $p<0.05$. Chi-square tests were carried out when comparing categorical data. Numerical data were tested first for their type of distributions. If data were distributed normally, unpaired Student t-tests were used to compare means between two groups and One Way ANOVA or Welch ANOVA

for larger groups, followed by post-doc Dunnett test for multiple comparisons to a fixed control. Two Way ANOVA was used when comparisons to two variables were made. If data were not normally distributed, non-parametric Mann-Whitney U-test for 2 two group comparisons and Kruskal Wallis ANOVA for larger groups, followed by post-hoc Dunn's multiple comparisons test to a fixed control. Statistical details including full genotypes, sample sizes, tests and p values are provided in Supplementary Table S2.

SUPPLEMENTARY TEXT

Supplementary Figure S2

The DNT-2 receptors *Toll-6* and *kek-6* are expressed in an associative circuit

Here we provide further details of the identification of cells expressing the DNT-2 receptors Toll-6 and Kek-6 in the adult brain:

1. *Toll6>FlyBow1.1* strongly labelled mushroom body (MB) lobes [48] (Figure 1H) and *kek-6>FlyBow1.1* did too (Figure 1I). To discern non-Kenyon cell projections of Toll-6+ or Kek-6+ neurons onto MB lobes, we combined *Toll6>FlyBow1.1* or *kek-6>FlyBow1.1* with *MB247-Gal80*, which inhibits Gal4 in Kenyon cells. This revealed Toll-6+ projections from PAM-α1, PAM-β2β'2 and PPL1-γped dopaminergic neurons (Figure S2A). In addition, we combined *Toll-6>CD8-RFP* with *R14C08-LexA>CD8-GFP* and co-localising signal showed that Mushroom Body Output Neuron (MBON)-M4M6 neurons are Toll-6+ as well (Figure S2C). Similarly, we identified Kek-6+ neuron projections from PPL1-γ2α'1 and/or MBON-γ2α'1 onto MB-γ2α'1, from PPL1-α2α'2 on MB α2α'2 and from PPL1-γped on MB-ped (Figure S2A,B).
2. We used MCFO to stochastically label *Toll-6* and *kek-6* expressing neurons. This revealed *Toll-6>MCFO+* αβ core, αβ surface and γ medial Kenyon Cells (Figure S2I); and *kek-6>MCFO+* αβ and α'β' Kenyon cells, as well as PPL1 γ2α'1 and α2α'2 neurons (Figure S2J). Using MCFO, we identified Kek-6+ single-cell clones as DAL neurons (Figure 1K, identified most likely as ID: 5813047772 using NeuPrint), meaning that *kek-6* is expressed in DAL neurons.

3. Expression from a DAL neuron reporter (*DAL-LexA>CD8-GFP*) colocalised with Toll-6 (*Toll-6GAL4>10xCD8-RFP*)(Figure S2G) and Kek-6 (*kek-6-6GAL4>10xCD8-RFP)* reporters (Figure S2H), demonstrating that DAL neurons express both *Toll-6* and *kek-6.*

4. Analysis of published single-cell RNAseq data [78, 134] confirmed our findings that multiple *Tolls, keks* and their downstream signalling effectors, are expressed in PAM, PAL and PPL1 dopaminergic neurons, Kenyon cells, DAL neurons and across all mushroom body output neuron types (Figure S2F, Supplementary Table S1).

In summary, the DNT-2 receptors Toll-6 and Kek-6 are expressed in Kenyon cells, DAN, DAL and MBONs.

REFERENCES

1. Bharmauria V, Ouelhazi A, Lussiez R, Molotchnikoff S. Adaptation-induced plasticity in the sensory cortex. J Neurophysiol. 2022;128(4):946-62. Epub 2022/09/22. doi: 10.1152/jn.00114.2022. PubMed PMID: 36130163.

2. Chen CC, Brumberg JC. Sensory Experience as a Regulator of Structural Plasticity in the Developing Whisker-to-Barrel System. Frontiers in Cellular Neuroscience. 2021;15. doi: ARTN 770453
10.3389/fncel.2021.770453. PubMed PMID: WOS:000741807500001.

3. Cheng LK, Chiu YH, Lin YC, Li WC, Hong TY, Yang CJ, et al. Long-term musical training induces white matter plasticity in emotion and language networks. Hum Brain Mapp. 2022. Epub 2022/08/26. doi: 10.1002/hbm.26054. PubMed PMID: 36005832.

4. Cotman CW, Berchtold NC. Exercise: a behavioral intervention to enhance brain health and plasticity. Trends in neurosciences. 2002;25(6):295-301. Epub 2002/06/28. doi: 10.1016/s0166-2236(02)02143-4. PubMed PMID: 12086747.

5. Feldman DE, Brecht M. Map plasticity in somatosensory cortex. Science. 2005;310(5749):810-5. Epub 2005/11/08. doi: 10.1126/science.1115807. PubMed PMID: 16272113.

6. Holtmaat A, Svoboda K. Experience-dependent structural synaptic plasticity in the mammalian brain. Nat Rev Neurosci. 2009;10(9):647-58. Epub 2009/08/21. doi: 10.1038/nrn2699. PubMed PMID: 19693029.

7. Sur M, Rubenstein JL. Patterning and plasticity of the cerebral cortex. Science. 2005;310(5749):805-10. Epub 2005/11/08. doi: 10.1126/science.1112070. PubMed PMID: 16272112.

8. Maguire EA, Gadian DG, Johnsrude IS, Good CD, Ashburner J, Frackowiak RS, et al. Navigation-related structural change in the hippocampi of taxi drivers. Proc Natl Acad Sci U S A. 2000;97(8):4398-403. Epub 2000/03/15. doi: 10.1073/pnas.070039597. PubMed PMID: 10716738; PubMed Central PMCID: PMCPMC18253.

9. Woollett K, Maguire EA. Acquiring "the Knowledge" of London's layout drives structural brain changes. Curr Biol. 2011;21(24):2109-14. Epub 2011/12/16. doi: 10.1016/j.cub.2011.11.018. PubMed PMID: 22169537; PubMed Central PMCID: PMCPMC3268356.

10. Kuner R, Flor H. Structural plasticity and reorganisation in chronic pain. Nat Rev Neurosci. 2016;18(1):20-30. Epub 2016/12/16. doi: 10.1038/nrn.2016.162. PubMed PMID: 27974843.

11. Leemhuis E, De Gennaro L, Pazzaglia AM. Disconnected Body Representation: Neuroplasticity Following Spinal Cord Injury. J Clin Med. 2019;8(12). Epub 2019/12/11. doi: 10.3390/jcm8122144. PubMed PMID: 31817187; PubMed Central PMCID: PMCPMC6947607.

12. Yang T, Nie Z, Shu H, Kuang Y, Chen X, Cheng J, et al. The Role of BDNF on Neural Plasticity in Depression. Front Cell Neurosci. 2020;14:82. Epub 2020/05/01. doi: 10.3389/fncel.2020.00082. PubMed PMID: 32351365; PubMed Central PMCID: PMCPMC7174655.

13. Castren E, Monteggia L. Brain-Derived Neurotrophic Factor Signaling in Depression and Antidepressant Action. Biol Psychiatry. 2021. Epub 2021/06/01. doi: 10.1016/j.biopsych.2021.05.008. PubMed PMID: 34053675.

14. Wohleb ES, Franklin T, Iwata M, Duman RS. Integrating neuroimmune systems in the neurobiology of depression. Nat Rev Neurosci. 2016;17(8):497-511. Epub 2016/06/10. doi: 10.1038/nrn.2016.69. PubMed PMID: 27277867.

15. Vahid-Ansari F, Albert PR. Rewiring of the Serotonin System in Major Depression. Front Psychiatry. 2021;12:802581. Epub 2022/01/04. doi: 10.3389/fpsyt.2021.802581. PubMed PMID: 34975594; PubMed Central PMCID: PMCPMC8716791.

16. Wang CS, Kavalali ET, Monteggia LM. BDNF signaling in context: From synaptic regulation to psychiatric disorders. Cell. 2022;185(1):62-76. Epub 2021/12/29. doi: 10.1016/j.cell.2021.12.003. PubMed PMID: 34963057; PubMed Central PMCID: PMCPMC8741740.

17. Lu B, Nagappan G, Guan X, Nathan PJ, Wren P. BDNF-based synaptic repair as a disease-modifying strategy for neurodegenerative diseases. Nat Rev Neurosci. 2013;14(6):401-16. Epub 2013/05/16. doi: nrn3505 [pii]
10.1038/nrn3505. PubMed PMID: 23674053.

18. Forrest MP, Parnell E, Penzes P. Dendritic structural plasticity and neuropsychiatric disease. Nat Rev Neurosci. 2018;19(4):215-34. Epub 2018/03/17. doi: 10.1038/nrn.2018.16. PubMed PMID: 29545546; PubMed Central PMCID: PMCPMC6442683.

19. Poo MM. Neurotrophins as synaptic modulators. Nat Rev Neurosci. 2001;2(1):24-32. Epub 2001/03/20. doi: 10.1038/35049004. PubMed PMID: 11253356.

20. Lu B, Pang PT, Woo NH. The yin and yang of neurotrophin action. Nat Rev Neurosci. 2005;6(8):603-14. Epub 2005/08/03. doi: 10.1038/nrn1726. PubMed PMID: 16062169.

21. Park H, Poo MM. Neurotrophin regulation of neural circuit development and function. Nat Rev Neurosci. 2013;14(1):7-23. Epub 2012/12/21. doi: 10.1038/nrn3379. PubMed PMID: 23254191.

22. Casarotto PC, Girych M, Fred SM, Kovaleva V, Moliner R, Enkavi G, et al. Antidepressant drugs act by directly binding to TRKB neurotrophin receptors. Cell. 2021;184(5):1299-313 e19. Epub 2021/02/20. doi: 10.1016/j.cell.2021.01.034. PubMed PMID: 33606976; PubMed Central PMCID: PMCPMC7938888.

23. Squillace S, Salvemini D. Toll-like receptor-mediated neuroinflammation: relevance for cognitive dysfunctions. Trends Pharmacol Sci. 2022;43(9):726-39. Epub 2022/06/27. doi: 10.1016/j.tips.2022.05.004. PubMed PMID: 35753845; PubMed Central PMCID: PMCPMC9378500.

24. Gay NJ, Gangloff M. Structure and function of Toll receptors and their ligands. Annu Rev Biochem. 2007;76:141-65. Epub 2007/03/17. doi: 10.1146/annurev.biochem.76.060305.151318. PubMed PMID: 17362201.

25. Ma Y, Li J, Chiu I, Wang Y, Sloane JA, Lu J, et al. Toll-like receptor 8 functions as a negative regulator of neurite outgrowth and inducer of neuronal apoptosis. J Cell Biol. 2006;175(2):209-15. Epub 2006/10/25. doi: 10.1083/jcb.200606016. PubMed PMID: 17060494; PubMed Central PMCID: PMCPMC2064562.

26. Okun E, Griffioen K, Barak B, Roberts NJ, Castro K, Pita MA, et al. Toll-like receptor 3 inhibits memory retention and constrains adult hippocampal neurogenesis. Proc Natl Acad Sci U S A. 2010;107(35):15625-30. Epub 2010/08/18. doi: 10.1073/pnas.1005807107. PubMed PMID: 20713712; PubMed Central PMCID: PMCPMC2932590.

27. Okun E, Griffioen KJ, Mattson MP. Toll-like receptor signaling in neural plasticity and disease. Trends in neurosciences. 2011;34(5):269-81. doi: 10.1016/j.tins.2011.02.005. PubMed PMID: 21419501; PubMed Central PMCID: PMC3095763.

28. Rolls A, Shechter R, London A, Ziv Y, Ronen A, Levy R, et al. Toll-like receptors modulate adult hippocampal neurogenesis. Nat Cell Biol. 2007;9(9):1081-8. Epub 2007/08/21. doi: 10.1038/ncb1629. PubMed PMID: 17704767.

29. Patel V, Patel AM, McArdle JJ. Synaptic abnormalities of mice lacking toll-like receptor (TLR)-9. Neuroscience. 2016;324:1-10. Epub 2016/03/10. doi: 10.1016/j.neuroscience.2016.03.001. PubMed PMID: 26955780.

30. Chen CY, Shih YC, Hung YF, Hsueh YP. Beyond defense: regulation of neuronal morphogenesis and brain functions via Toll-like receptors. J Biomed Sci. 2019;26(1):90. Epub 2019/11/07. doi: 10.1186/s12929-019-0584-z. PubMed PMID: 31684953; PubMed Central PMCID: PMCPMC6827257.

31. Barth M, Heisenberg M. Vision affects mushroom bodies and central complex in Drosophila melanogaster. Learn Mem. 1997;4(2):219-29. Epub 1997/07/01. doi: 10.1101/lm.4.2.219. PubMed PMID: 10456065.

32. Barth M, Hirsch HV, Meinertzhagen IA, Heisenberg M. Experience-dependent developmental plasticity in the optic lobe of Drosophila melanogaster. J Neurosci. 1997;17(4):1493-504. Epub 1997/02/15. PubMed PMID: 9006990; PubMed Central PMCID: PMCPMC6793721.

33. Heisenberg M, Heusipp M, Wanke C. Structural plasticity in the Drosophila brain. J Neurosci. 1995;15(3 Pt 1):1951-60. Epub 1995/03/01. PubMed PMID: 7891144; PubMed Central PMCID: PMCPMC6578107.

34. Baltruschat L, Prisco L, Ranft P, Lauritzen JS, Fiala A, Bock DD, et al. Circuit reorganization in the Drosophila mushroom body calyx accompanies memory consolidation. Cell Rep. 2021;34(11):108871. Epub 2021/03/18. doi: 10.1016/j.celrep.2021.108871. PubMed PMID: 33730583.

35. Kremer MC, Christiansen F, Leiss F, Paehler M, Knapek S, Andlauer TF, et al. Structural long-term changes at mushroom body input synapses. Curr Biol. 2010;20(21):1938-44. Epub 2010/10/19. doi: 10.1016/j.cub.2010.09.060. PubMed PMID: 20951043.

36. Sugie A, Hakeda-Suzuki S, Suzuki E, Silies M, Shimozono M, Mohl C, et al. Molecular Remodeling of the Presynaptic Active Zone of Drosophila Photoreceptors via Activity-Dependent Feedback. Neuron. 2015;86(3):711-25. Epub 2015/04/22. doi: 10.1016/j.neuron.2015.03.046. PubMed PMID: 25892303.

37. Linneweber GA, Andriatsilavo M, Dutta SB, Bengochea M, Hellbruegge L, Liu G, et al. A neurodevelopmental origin of behavioral individuality in the Drosophila visual system. Science. 2020;367(6482):1112-9. Epub 2020/03/07. doi: 10.1126/science.aaw7182. PubMed PMID: 32139539.

38. Sugie A, Marchetti G, Tavosanis G. Structural aspects of plasticity in the nervous system of Drosophila. Neural Dev. 2018;13(1):14. Epub 2018/07/02. doi: 10.1186/s13064-018-0111-z. PubMed PMID: 29960596; PubMed Central PMCID: PMCPMC6026517.

39. Sachse S, Rueckert E, Keller A, Okada R, Tanaka NK, Ito K, et al. Activity-dependent plasticity in an olfactory circuit. Neuron. 2007;56(5):838-50. Epub 2007/12/07. doi: 10.1016/j.neuron.2007.10.035. PubMed PMID: 18054860.

40. Technau GM. Fiber number in the mushroom bodies of adult Drosophila melanogaster depends on age, sex and experience. J Neurogenet. 1984;1(2):113-26. Epub 1984/04/01. doi: 10.3109/01677068409107077. PubMed PMID: 6085635.

41. Devaud JM, Acebes A, Ferrus A. Odor exposure causes central adaptation and morphological changes in selected olfactory glomeruli in Drosophila. J Neurosci. 2001;21(16):6274-82. Epub 2001/08/07. PubMed PMID: 11487650; PubMed Central PMCID: PMCPMC6763130.

42. Gorska-Andrzejak J, Keller A, Raabe T, Kilianek L, Pyza E. Structural daily rhythms in GFP-labelled neurons in the visual system of Drosophila melanogaster. Photochem Photobiol Sci. 2005;4(9):721-6. Epub 2005/08/27. doi: 10.1039/b417023g. PubMed PMID: 16121283.

43. Bushey D, Tononi G, Cirelli C. Sleep and synaptic homeostasis: structural evidence in Drosophila. Science. 2011;332(6037):1576-81. Epub 2011/06/28. doi: 10.1126/science.1202839. PubMed PMID: 21700878; PubMed Central PMCID: PMCPMC3128387.

44. Vaughen JP, Theisen E, Rivas-Serna IM, Berger AB, Kalakuntla P, Anreiter I, et al. Glial control of sphingolipid levels sculpts diurnal remodeling in a circadian circuit. Neuron. 2022;110(19):3186-205 e7. Epub 2022/08/13. doi: 10.1016/j.neuron.2022.07.016. PubMed PMID: 35961319.

45. Fernandez MP, Berni J, Ceriani MF. Circadian remodeling of neuronal circuits involved in rhythmic behavior. PLoS Biol. 2008;6(3):e69. Epub 2008/03/28. doi: 10.1371/journal.pbio.0060069. PubMed PMID: 18366255; PubMed Central PMCID: PMCPMC2270325.

46. Duhart JM, Herrero A, de la Cruz G, Ispizua JI, Pirez N, Ceriani MF. Circadian Structural Plasticity Drives Remodeling of E Cell Output. Curr Biol. 2020;30(24):5040-8 e5. Epub 2020/10/17. doi: 10.1016/j.cub.2020.09.057. PubMed PMID: 33065014.

47. Bolus H, Crocker K, Boekhoff-Falk G, Chtarbanova S. Modeling Neurodegenerative Disorders in Drosophila melanogaster. Int J Mol Sci. 2020;21(9). Epub 2020/05/03. doi: 10.3390/ijms21093055. PubMed PMID: 32357532; PubMed Central PMCID: PMCPMC7246467.

48. Li G, Forero MG, Wentzell JS, Durmus I, Wolf R, Anthoney NC, et al. A Toll-receptor map underlies structural brain plasticity. Elife. 2020;9. Epub 2020/02/19. doi: 10.7554/eLife.52743. PubMed PMID: 32066523; PubMed Central PMCID: PMCPMC7077983.

49. Anthoney N, Foldi I, Hidalgo A. Toll and Toll-like receptor signalling in development. Development. 2018;145(9). Epub 2018/04/27. doi: 10.1242/dev.156018. PubMed PMID: 29695493.

50. Foldi I, Anthoney N, Harrison N, Gangloff M, Verstak B, Nallasivan MP, et al. Three-tier regulation of cell number plasticity by neurotrophins and Tolls in Drosophila. J Cell Biol. 2017;216(5):1421-38. Epub 2017/04/05. doi: 10.1083/jcb.201607098. PubMed PMID: 28373203; PubMed Central PMCID: PMCPMC5412559.

51. McIlroy G, Foldi I, Aurikko J, Wentzell JS, Lim MA, Fenton JC, et al. Toll-6 and Toll-7 function as neurotrophin receptors in the Drosophila melanogaster CNS. Nat Neurosci. 2013;16(9):1248-56. Epub 2013/07/31. doi: 10.1038/nn.3474. PubMed PMID: 23892553; PubMed Central PMCID: PMCPMC4634317.

52. Meyer SN, Amoyel M, Bergantinos C, de la Cova C, Schertel C, Basler K, et al. An ancient defense system eliminates unfit cells from developing tissues during cell competition. Science. 2014;346(6214):1258236. doi: 10.1126/science.1258236. PubMed PMID: 25477468; PubMed Central PMCID: PMCPMC5095928.

53. Pare AC, Vichas A, Fincher CT, Mirman Z, Farrell DL, Mainieri A, et al. A positional Toll receptor code directs convergent extension in Drosophila. Nature. 2014;515(7528):523-7. Epub 2014/11/05. doi: 10.1038/nature13953. PubMed PMID: 25363762; PubMed Central PMCID: PMCPMC4943584.

54. Tamada M, Shi J, Bourdot KS, Supriyatno S, Palmquist KH, Gutierrez-Ruiz OL, et al. Toll receptors remodel epithelia by directing planar-polarized Src and PI3K activity. Dev Cell.

2021;56(11):1589-602 e9. Epub 2021/05/02. doi: 10.1016/j.devcel.2021.04.012. PubMed PMID: 33932332; PubMed Central PMCID: PMCPMC8570296.

55. Ward A, Hong W, Favaloro V, Luo L. Toll receptors instruct axon and dendrite targeting and participate in synaptic partner matching in a Drosophila olfactory circuit. Neuron. 2015;85(5):1013-28. Epub 2015/03/06. doi: 10.1016/j.neuron.2015.02.003. PubMed PMID: 25741726; PubMed Central PMCID: PMCPMC4351475.

56. McLaughlin CN, Nechipurenko IV, Liu N, Broihier HT. A Toll receptor-FoxO pathway represses Pavarotti/MKLP1 to promote microtubule dynamics in motoneurons. J Cell Biol. 2016;214(4):459-74. Epub 2016/08/10. doi: 10.1083/jcb.201601014. PubMed PMID: 27502486; PubMed Central PMCID: PMCPMC4987293.

57. Riemensperger T, Isabel G, Coulom H, Neuser K, Seugnet L, Kume K, et al. Behavioral consequences of dopamine deficiency in the Drosophila central nervous system. Proc Natl Acad Sci U S A. 2011;108(2):834-9. doi: 10.1073/pnas.1010930108. PubMed PMID: 21187381; PubMed Central PMCID: PMCPMC3021077.

58. Waddell S. Reinforcement signalling in Drosophila; dopamine does it all after all. Curr Opin Neurobiol. 2013;23(3):324-9. Epub 2013/02/09. doi: 10.1016/j.conb.2013.01.005. PubMed PMID: 23391527; PubMed Central PMCID: PMCPMC3887340.

59. Waddell S. Dopamine reveals neural circuit mechanisms of fly memory. Trends in neurosciences. 2010;33(10):457-64. Epub 2010/08/13. doi: 10.1016/j.tins.2010.07.001. PubMed PMID: 20701984; PubMed Central PMCID: PMCPMC2947577.

60. Yamagata N, Ichinose T, Aso Y, Placais PY, Friedrich AB, Sima RJ, et al. Distinct dopamine neurons mediate reward signals for short- and long-term memories. Proc Natl Acad Sci U S A. 2015;112(2):578-83. Epub 2014/12/31. doi: 10.1073/pnas.1421930112. PubMed PMID: 25548178; PubMed Central PMCID: PMCPMC4299218.

61. Adel M, Griffith LC. The Role of Dopamine in Associative Learning in Drosophila: An Updated Unified Model. Neurosci Bull. 2021;37(6):831-52. Epub 2021/03/30. doi: 10.1007/s12264-021-00665-0. PubMed PMID: 33779893; PubMed Central PMCID: PMCPMC8192648.

62. Aso Y, Hattori D, Yu Y, Johnston RM, Iyer NA, Ngo TT, et al. The neuronal architecture of the mushroom body provides a logic for associative learning. Elife. 2014;3:e04577. Epub 2014/12/24. doi: 10.7554/eLife.04577. PubMed PMID: 25535793; PubMed Central PMCID: PMCPMC4273437.

63. Chen CC, Wu JK, Lin HW, Pai TP, Fu TF, Wu CL, et al. Visualizing long-term memory formation in two neurons of the Drosophila brain. Science. 2012;335(6069):678-85. Epub 2012/02/11. doi: 10.1126/science.1212735. PubMed PMID: 22323813.

64. Krashes MJ, Waddell S. Rapid consolidation to a radish and protein synthesis-dependent long-term memory after single-session appetitive olfactory conditioning in Drosophila. J Neurosci. 2008;28(12):3103-13. Epub 2008/03/21. doi: 10.1523/JNEUROSCI.5333-07.2008. PubMed PMID: 18354013; PubMed Central PMCID: PMCPMC2516741.

65. Placais PY, Trannoy S, Isabel G, Aso Y, Siwanowicz I, Belliart-Guerin G, et al. Slow oscillations in two pairs of dopaminergic neurons gate long-term memory formation in Drosophila. Nat Neurosci. 2012;15(4):592-9. Epub 2012/03/01. doi: 10.1038/nn.3055. PubMed PMID: 22366756.

66. Guven-Ozkan T, Davis RL. Functional neuroanatomy of Drosophila olfactory memory formation. Learn Mem. 2014;21(10):519-26. Epub 2014/09/17. doi: 10.1101/lm.034363.114. PubMed PMID: 25225297; PubMed Central PMCID: PMCPMC4175493.

67. Weber AN, Tauszig-Delamasure S, Hoffmann JA, Lelievre E, Gascan H, Ray KP, et al. Binding of the Drosophila cytokine Spatzle to Toll is direct and establishes signaling. Nat Immunol. 2003;4(8):794-800. doi: 10.1038/ni955. PubMed PMID: 12872120.

68. Hoffmann A, Funkner A, Neumann P, Juhnke S, Walther M, Schierhorn A, et al. Biophysical characterization of refolded Drosophila Spatzle, a cystine knot protein, reveals distinct properties of three isoforms. J Biol Chem. 2008;283(47):32598-609. Epub 2008/09/16. doi: 10.1074/jbc.M801815200. PubMed PMID: 18790733.

69. Hoffmann A, Neumann P, Schierhorn A, Stubbs MT. Crystallization of Spatzle, a cystine-knot protein involved in embryonic development and innate immunity in Drosophila melanogaster. Acta Crystallogr Sect F Struct Biol Cryst Commun. 2008;64(Pt 8):707-10. Epub 2008/08/06. doi: 10.1107/S1744309108018812. PubMed PMID: 18678937; PubMed Central PMCID: PMCPMC2494967.

70. Lewis M, Arnot CJ, Beeston H, McCoy A, Ashcroft AE, Gay NJ, et al. Cytokine Spatzle binds to the Drosophila immunoreceptor Toll with a neurotrophin-like specificity and couples receptor activation. Proc Natl Acad Sci U S A. 2013;110(51):20461-6. Epub 2013/11/28. doi: 10.1073/pnas.1317002110. PubMed PMID: 24282309; PubMed Central PMCID: PMCPMC3870763.

71. DeLotto Y, DeLotto R. Proteolytic processing of the Drosophila Spatzle protein by easter generates a dimeric NGF-like molecule with ventralising activity. Mech Dev. 1998;72(1-2):141-8. Epub 1998/05/12. doi: 10.1016/s0925-4773(98)00024-0. PubMed PMID: 9533958.

72. Zhu B, Pennack JA, McQuilton P, Forero MG, Mizuguchi K, Sutcliffe B, et al. Drosophila neurotrophins reveal a common mechanism for nervous system formation. PLoS Biol. 2008;6(11):e284. doi: 10.1371/journal.pbio.0060284. PubMed PMID: 19018662; PubMed Central PMCID: PMCPMC2586362.

73. Sutcliffe B, Forero MG, Zhu B, Robinson IM, Hidalgo A. Neuron-type specific functions of DNT1, DNT2 and Spz at the Drosophila neuromuscular junction. PLoS One. 2013;8(10):e75902. Epub 2013/10/15. doi: 10.1371/journal.pone.0075902. PubMed PMID: 24124519; PubMed Central PMCID: PMCPMC3790821.

74. Ulian-Benitez S, Bishop S, Foldi I, Wentzell J, Okenwa C, Forero MG, et al. Kek-6: A truncated-Trk-like receptor for Drosophila neurotrophin 2 regulates structural synaptic plasticity. PLoS Genet. 2017;13(8):e1006968. Epub 2017/08/29. doi: 10.1371/journal.pgen.1006968. PubMed PMID: 28846707; PubMed Central PMCID: PMCPMC5591008.

75. Costa M, Manton JD, Ostrovsky AD, Prohaska S, Jefferis GS. NBLAST: Rapid, Sensitive Comparison of Neuronal Structure and Construction of Neuron Family Databases. Neuron.

2016;91(2):293-311. Epub 2016/07/05. doi: 10.1016/j.neuron.2016.06.012. PubMed PMID: 27373836; PubMed Central PMCID: PMCPMC4961245.

76. Nern A, Pfeiffer BD, Rubin GM. Optimized tools for multicolor stochastic labeling reveal diverse stereotyped cell arrangements in the fly visual system. Proc Natl Acad Sci U S A. 2015;112(22):E2967-76. Epub 2015/05/13. doi: 10.1073/pnas.1506763112. PubMed PMID: 25964354; PubMed Central PMCID: PMCPMC4460454.

77. Mayseless O, Berns DS, Yu XM, Riemensperger T, Fiala A, Schuldiner O. Developmental Coordination during Olfactory Circuit Remodeling in Drosophila. Neuron. 2018;99(6):1204-15 e5. Epub 2018/08/28. doi: 10.1016/j.neuron.2018.07.050. PubMed PMID: 30146303.

78. Croset V, Treiber CD, Waddell S. Cellular diversity in the Drosophila midbrain revealed by single-cell transcriptomics. Elife. 2018;7. Epub 2018/04/20. doi: 10.7554/eLife.34550. PubMed PMID: 29671739; PubMed Central PMCID: PMCPMC5927767.

79. Cervantes-Sandoval I, Phan A, Chakraborty M, Davis RL. Reciprocal synapses between mushroom body and dopamine neurons form a positive feedback loop required for learning. Elife. 2017;6. Epub 2017/05/11. doi: 10.7554/eLife.23789. PubMed PMID: 28489528; PubMed Central PMCID: PMCPMC5425253.

80. Talay M, Richman EB, Snell NJ, Hartmann GG, Fisher JD, Sorkac A, et al. Transsynaptic Mapping of Second-Order Taste Neurons in Flies by trans-Tango. Neuron. 2017;96(4):783-95 e4. Epub 2017/11/07. doi: 10.1016/j.neuron.2017.10.011. PubMed PMID: 29107518; PubMed Central PMCID: PMCPMC5693608.

81. Cachero S, Gkantia M, Bates AS, Frechter S, Blackie L, McCarthy A, et al. BAcTrace a new tool for retrograde tracing of neuronal circuit. Nature Methods. 2020;17:1254-61. doi: 10.1101/2020.01.24.918656.

82. Martin-Blanco E, Gampel A, Ring J, Virdee K, Kirov N, Tolkovsky AM, et al. puckered encodes a phosphatase that mediates a feedback loop regulating JNK activity during dorsal closure in Drosophila. Genes Dev. 1998;12(4):557-70. PubMed PMID: 9472024; PubMed Central PMCID: PMCPMC316530.

83. Neve KA, Seamans JK, Trantham-Davidson H. Dopamine receptor signaling. J Recept Signal Transduct Res. 2004;24(3):165-205. Epub 2004/11/04. doi: 10.1081/rrs-200029981. PubMed PMID: 15521361.

84. Hearn MG, Ren Y, McBride EW, Reveillaud I, Beinborn M, Kopin AS. A Drosophila dopamine 2-like receptor: Molecular characterization and identification of multiple alternatively spliced variants. Proc Natl Acad Sci U S A. 2002;99(22):14554-9. Epub 2002/10/23. doi: 10.1073/pnas.202498299. PubMed PMID: 12391323; PubMed Central PMCID: PMCPMC137921.

85. Shafer OT, Kim DJ, Dunbar-Yaffe R, Nikolaev VO, Lohse MJ, Taghert PH. Widespread receptivity to neuropeptide PDF throughout the neuronal circadian clock network of Drosophila revealed by real-time cyclic AMP imaging. Neuron. 2008;58(2):223-37. Epub 2008/04/29. doi: 10.1016/j.neuron.2008.02.018. PubMed PMID: 18439407; PubMed Central PMCID: PMCPMC2586874.

86. Liu C, Placais PY, Yamagata N, Pfeiffer BD, Aso Y, Friedrich AB, et al. A subset of dopamine neurons signals reward for odour memory in Drosophila. Nature. 2012;488(7412):512-6. Epub 2012/07/20. doi: 10.1038/nature11304. PubMed PMID: 22810589.

87. Feany MB, Bender WW. A Drosophila model of Parkinson's disease. Nature. 2000;404(6776):394-8. doi: 10.1038/35006074. PubMed PMID: 10746727.

88. Aso Y, Herb A, Ogueta M, Siwanowicz I, Templier T, Friedrich AB, et al. Three dopamine pathways induce aversive odor memories with different stability. PLoS Genet. 2012;8(7):e1002768. Epub 2012/07/19. doi: 10.1371/journal.pgen.1002768. PubMed PMID: 22807684; PubMed Central PMCID: PMCPMC3395599.

89. Aso Y, Siwanowicz I, Bracker L, Ito K, Kitamoto T, Tanimoto H. Specific dopaminergic neurons for the formation of labile aversive memory. Curr Biol. 2010;20(16):1445-51. Epub 2010/07/20. doi: 10.1016/j.cub.2010.06.048. PubMed PMID: 20637624; PubMed Central PMCID: PMCPMC2929706.

90. Scheunemann L, Placais PY, Dromard Y, Schwarzel M, Preat T. Dunce Phosphodiesterase Acts as a Checkpoint for Drosophila Long-Term Memory in a Pair of Serotonergic Neurons. Neuron. 2018;98(2):350-65 e5. Epub 2018/04/21. doi: 10.1016/j.neuron.2018.03.032. PubMed PMID: 29673482; PubMed Central PMCID: PMCPMC5919781.

91. Pech U, Revelo NH, Seitz KJ, Rizzoli SO, Fiala A. Optical dissection of experience-dependent pre- and postsynaptic plasticity in the Drosophila brain. Cell Rep. 2015;10(12):2083-95. Epub 2015/03/31. doi: 10.1016/j.celrep.2015.02.065. PubMed PMID: 25818295.

92. Fuentes-Medel Y, Logan MA, Ashley J, Ataman B, Budnik V, Freeman MR. Glia and muscle sculpt neuromuscular arbors by engulfing destabilized synaptic boutons and shed presynaptic debris. PLoS Biol. 2009;7(8):e1000184. Epub 2009/08/27. doi: 10.1371/journal.pbio.1000184. PubMed PMID: 19707574; PubMed Central PMCID: PMCPMC2724735.

93. Tripodi M, Evers JF, Mauss A, Bate M, Landgraf M. Structural homeostasis: compensatory adjustments of dendritic arbor geometry in response to variations of synaptic input. PLoS Biol. 2008;6(10):e260. Epub 2008/10/31. doi: 10.1371/journal.pbio.0060260. PubMed PMID: 18959482; PubMed Central PMCID: PMCPMC2573934.

94. Jenks KR, Tsimring K, Ip JPK, Zepeda JC, Sur M. Heterosynaptic Plasticity and the Experience-Dependent Refinement of Developing Neuronal Circuits. Front Neural Circuits. 2021;15:803401. Epub 2021/12/25. doi: 10.3389/fncir.2021.803401. PubMed PMID: 34949992; PubMed Central PMCID: PMCPMC8689143.

95. Riemensperger T, Issa AR, Pech U, Coulom H, Nguyen MV, Cassar M, et al. A single dopamine pathway underlies progressive locomotor deficits in a Drosophila model of Parkinson disease. Cell Rep. 2013;5(4):952-60. doi: 10.1016/j.celrep.2013.10.032. PubMed PMID: 24239353.

96. Sun J, Xu AQ, Giraud J, Poppinga H, Riemensperger T, Fiala A, et al. Neural Control of Startle-Induced Locomotion by the Mushroom Bodies and Associated Neurons in Drosophila. Front Syst Neurosci. 2018;12:6. Epub 2018/04/13. doi: 10.3389/fnsys.2018.00006. PubMed PMID: 29643770; PubMed Central PMCID: PMCPMC5882849.

97. Eyjolfsdottir E, Branson S, Burgos-Artizzu XP, Hoopfer ED, Schor J, Anderson DJ, et al., editors. Detecting Social Actions of Fruit Flies2014; Cham: Springer International Publishing.

98. Krashes MJ, Waddell S. Drosophila appetitive olfactory conditioning. Cold Spring Harb Protoc. 2011;2011(5):pdb prot5609. Epub 2011/05/04. doi: 10.1101/pdb.prot5609. PubMed PMID: 21536767.

99. Mandai K, Guo T, St Hillaire C, Meabon JS, Kanning KC, Bothwell M, et al. LIG family receptor tyrosine kinase-associated proteins modulate growth factor signals during neural development. Neuron. 2009;63(5):614-27. Epub 2009/09/17. doi: 10.1016/j.neuron.2009.07.031. PubMed PMID: 19755105; PubMed Central PMCID: PMCPMC2758028.

100. MacLaren CM, Evans TA, Alvarado D, Duffy JB. Comparative analysis of the Kekkon molecules, related members of the LIG superfamily. Dev Genes Evol. 2004;214(7):360-6. Epub 2004/06/05. doi: 10.1007/s00427-004-0414-4. PubMed PMID: 15179511.

101. Tauszig S, Jouanguy E, Hoffmann JA, Imler JL. Toll-related receptors and the control of antimicrobial peptide expression in Drosophila. Proc Natl Acad Sci U S A. 2000;97(19):10520-5. Epub 2000/09/06. doi: 10.1073/pnas.180130797. PubMed PMID: 10973475; PubMed Central PMCID: PMCPMC27057.

102. Arnot CJ, Gay NJ, Gangloff M. Molecular mechanism that induces activation of Spatzle, the ligand for the Drosophila Toll receptor. J Biol Chem. 2010;285(25):19502-9. Epub 2010/04/10. doi: 10.1074/jbc.M109.098186. PubMed PMID: 20378549; PubMed Central PMCID: PMCPMC2885229.

103. Hu X, Yagi Y, Tanji T, Zhou S, Ip YT. Multimerization and interaction of Toll and Spatzle in Drosophila. Proc Natl Acad Sci U S A. 2004;101(25):9369-74. Epub 2004/06/16. doi: 10.1073/pnas.0307062101. PubMed PMID: 15197269; PubMed Central PMCID: PMCPMC438983.

104. Arikkath J. Molecular mechanisms of dendrite morphogenesis. Front Cell Neurosci. 2012;6:61. Epub 2013/01/08. doi: 10.3389/fncel.2012.00061. PubMed PMID: 23293584; PubMed Central PMCID: PMCPMC3531598.

105. Horch HW, Katz LC. BDNF release from single cells elicits local dendritic growth in nearby neurons. Nat Neurosci. 2002;5(11):1177-84. Epub 2002/10/09. doi: 10.1038/nn927. PubMed PMID: 12368805.

106. Leiss F, Koper E, Hein I, Fouquet W, Lindner J, Sigrist S, et al. Characterization of dendritic spines in the Drosophila central nervous system. Dev Neurobiol. 2009;69(4):221-34. Epub 2009/01/23. doi: 10.1002/dneu.20699. PubMed PMID: 19160442.

107. Minichiello L. TrkB signalling pathways in LTP and learning. Nat Rev Neurosci. 2009;10(12):850-60. Epub 2009/11/21. doi: 10.1038/nrn2738. PubMed PMID: 19927149.

108. Lee JL, Everitt BJ, Thomas KL. Independent cellular processes for hippocampal memory consolidation and reconsolidation. Science. 2004;304(5672):839-43. Epub 2004/04/10. doi: 10.1126/science.1095760. PubMed PMID: 15073322.

109. Blochl A, Sirrenberg C. Neurotrophins stimulate the release of dopamine from rat mesencephalic neurons via Trk and p75Lntr receptors. J Biol Chem. 1996;271(35):21100-7. Epub 1996/08/30. doi: 10.1074/jbc.271.35.21100. PubMed PMID: 8702878.

110. Guillin O, Diaz J, Carroll P, Griffon N, Schwartz JC, Sokoloff P. BDNF controls dopamine D3 receptor expression and triggers behavioural sensitization. Nature. 2001;411(6833):86-9. Epub 2001/05/03. doi: 10.1038/35075076. PubMed PMID: 11333982.

111. Sahu MP, Pazos-Boubeta Y, Pajanoja C, Rozov S, Panula P, Castren E. Neurotrophin receptor Ntrk2b function in the maintenance of dopamine and serotonin neurons in zebrafish. Sci Rep. 2019;9(1):2036. Epub 2019/02/16. doi: 10.1038/s41598-019-39347-3. PubMed PMID: 30765816; PubMed Central PMCID: PMCPMC6375947.

112. Hyman C, Hofer M, Barde YA, Juhasz M, Yancopoulos GD, Squinto SP, et al. BDNF is a neurotrophic factor for dopaminergic neurons of the substantia nigra. Nature. 1991;350(6315):230-2. Epub 1991/03/21. doi: 10.1038/350230a0. PubMed PMID: 2005978.

113. Berton O, McClung CA, Dileone RJ, Krishnan V, Renthal W, Russo SJ, et al. Essential role of BDNF in the mesolimbic dopamine pathway in social defeat stress. Science. 2006;311(5762):864-8. Epub 2006/02/14. doi: 10.1126/science.1120972. PubMed PMID: 16469931.

114. Stoilov P, Castren E, Stamm S. Analysis of the human TrkB gene genomic organization reveals novel TrkB isoforms, unusual gene length, and splicing mechanism. Biochem Biophys Res Commun. 2002;290(3):1054-65. Epub 2002/01/19. doi: 10.1006/bbrc.2001.6301. PubMed PMID: 11798182.

115. Fryer RH, Kaplan DR, Feinstein SC, Radeke MJ, Grayson DR, Kromer LF. Developmental and mature expression of full-length and truncated TrkB receptors in the rat forebrain. J Comp Neurol. 1996;374(1):21-40. Epub 1996/10/07. doi: 10.1002/(SICI)1096-9861(19961007)374:1<21::AID-CNE2>3.0.CO;2-P. PubMed PMID: 8891944.

116. Yacoubian TA, Lo DC. Truncated and full-length TrkB receptors regulate distinct modes of dendritic growth. Nat Neurosci. 2000;3(4):342-9. Epub 2000/03/22. doi: 10.1038/73911. PubMed PMID: 10725923.

117. Tessarollo L, Yanpallewar S. TrkB Truncated Isoform Receptors as Transducers and Determinants of BDNF Functions. Front Neurosci. 2022;16:847572. Epub 2022/03/25. doi: 10.3389/fnins.2022.847572. PubMed PMID: 35321093; PubMed Central PMCID: PMCPMC8934854.

118. Fenner BM. Truncated TrkB: beyond a dominant negative receptor. Cytokine Growth Factor Rev. 2012;23(1-2):15-24. Epub 2012/02/22. doi: S1359-6101(12)00003-2 [pii] 10.1016/j.cytogfr.2012.01.002. PubMed PMID: 22341689.

119. Ohira K, Hayashi M. A new aspect of the TrkB signaling pathway in neural plasticity. Curr Neuropharmacol. 2009;7(4):276-85. Epub 2010/06/02. doi: 10.2174/157015909790031210. PubMed PMID: 20514207; PubMed Central PMCID: PMC2811861.

120. Ferrer I, Marin C, Rey MJ, Ribalta T, Goutan E, Blanco R, et al. BDNF and full-length and truncated TrkB expression in Alzheimer disease. Implications in therapeutic strategies. J Neuropathol Exp Neurol. 1999;58(7):729-39. PubMed PMID: 10411343.

121. Carim-Todd L, Bath KG, Fulgenzi G, Yanpallewar S, Jing D, Barrick CA, et al. Endogenous truncated TrkB.T1 receptor regulates neuronal complexity and TrkB kinase receptor function in vivo. J Neurosci. 2009;29(3):678-85. Epub 2009/01/23. doi: 10.1523/JNEUROSCI.5060-08.2009. PubMed PMID: 19158294; PubMed Central PMCID: PMCPMC2719435.

122. Ernst C, Deleva V, Deng X, Sequeira A, Pomarenski A, Klempan T, et al. Alternative splicing, methylation state, and expression profile of tropomyosin-related kinase B in the frontal cortex of suicide completers. Arch Gen Psychiatry. 2009;66(1):22-32. Epub 2009/01/07. doi: 10.1001/archpsyc.66.1.22. PubMed PMID: 19124685.

123. Ohira K, Homma KJ, Hirai H, Nakamura S, Hayashi M. TrkB-T1 regulates the RhoA signaling and actin cytoskeleton in glioma cells. Biochem Biophys Res Commun. 2006;342(3):867-74. Epub 2006/02/28. doi: 10.1016/j.bbrc.2006.02.033. PubMed PMID: 16500620.

124. Adhikarla SV, Jha NK, Goswami VK, Sharma A, Bhardwaj A, Dey A, et al. TLR-Mediated Signal Transduction and Neurodegenerative Disorders. Brain Sci. 2021;11(11). Epub 2021/11/28. doi: 10.3390/brainsci11111373. PubMed PMID: 34827372; PubMed Central PMCID: PMCPMC8615980.

125. Figueroa-Hall LK, Paulus MP, Savitz J. Toll-Like Receptor Signaling in Depression. Psychoneuroendocrinology. 2020;121:104843. Epub 2020/09/11. doi: 10.1016/j.psyneuen.2020.104843. PubMed PMID: 32911436; PubMed Central PMCID: PMCPMC7883590.

126. Sharma A. Genome-wide expression analysis in epilepsy: a synthetic review. Curr Top Med Chem. 2012;12(9):1008-32. Epub 2012/02/23. doi: 10.2174/156802612800229189. PubMed PMID: 22352865.

127. Chan RF, Turecki G, Shabalin AA, Guintivano J, Zhao M, Xie LY, et al. Cell Type-Specific Methylome-wide Association Studies Implicate Neurotrophin and Innate Immune Signaling in Major Depressive Disorder. Biol Psychiatry. 2020;87(5):431-42. Epub 2020/01/01. doi: 10.1016/j.biopsych.2019.10.014. PubMed PMID: 31889537.

128. Garrett ME, Qin XJ, Mehta D, Dennis MF, Marx CE, Grant GA, et al. Gene Expression Analysis in Three Posttraumatic Stress Disorder Cohorts Implicates Inflammation and Innate Immunity Pathways and Uncovers Shared Genetic Risk With Major Depressive Disorder. Front Neurosci. 2021;15:678548. Epub 2021/08/17. doi: 10.3389/fnins.2021.678548. PubMed PMID: 34393704; PubMed Central PMCID: PMCPMC8358297.

129. Mehta D, Voisey J, Bruenig D, Harvey W, Morris CP, Lawford B, et al. Transcriptome analysis reveals novel genes and immune networks dysregulated in veterans with PTSD. Brain Behav Immun. 2018;74:133-42. Epub 2018/09/07. doi: 10.1016/j.bbi.2018.08.014. PubMed PMID: 30189241.

130. Krishnan V, Nestler EJ. The molecular neurobiology of depression. Nature. 2008;455(7215):894-902. Epub 2008/10/17. doi: 10.1038/nature07455. PubMed PMID: 18923511; PubMed Central PMCID: PMCPMC2721780.

131. Martinowich K, Manji H, Lu B. New insights into BDNF function in depression and anxiety. Nat Neurosci. 2007;10(9):1089-93. Epub 2007/08/30. doi: 10.1038/nn1971. PubMed PMID: 17726474.

132. Yamazaki D, Hiroi M, Abe T, Shimizu K, Minami-Ohtsubo M, Maeyama Y, et al. Two Parallel Pathways Assign Opposing Odor Valences during Drosophila Memory Formation. Cell Rep. 2018;22(9):2346-58. Epub 2018/03/01. doi: 10.1016/j.celrep.2018.02.012. PubMed PMID: 29490271.

133. Ostrovsky A, Cachero S, Jefferis G. Clonal analysis of olfaction in Drosophila: image registration. Cold Spring Harb Protoc. 2013;2013(4):347-9. Epub 2013/04/03. doi: 10.1101/pdb.prot071738. PubMed PMID: 23547150.

134. Crocker A, Guan XJ, Murphy CT, Murthy M. Cell-Type-Specific Transcriptome Analysis in the Drosophila Mushroom Body Reveals Memory-Related Changes in Gene Expression. Cell Rep. 2016;15(7):1580-96. Epub 2016/05/11. doi: 10.1016/j.celrep.2016.04.046. PubMed PMID: 27160913; PubMed Central PMCID: PMCPMC5047377.

FIGURE LEGENDS

Figure 1 Neurons expressing *DNT-2* and its receptors *Toll-6* and *kek-6* in the adult brain

(A) *DNT-2A* expressing neurons (*DNT-2>FlyBow1.1* in green; anti-Brp in magenta) have cell bodies in SOG and project to FLA/PRW and SMP. **(B,D)** Pre-synaptic (green) and post-synaptic (magenta) terminals of DNT-2A neurons seen with *DNT-2>DenMark::RFP, Dsyd1::GFP*, higher magnification in **(D),** different specimens from (B). DNT-2A projections at SMP and PRW have both pre- and post-synaptic sites. **(C)** Single neuron DNT-2A>MCFO clones. **(E)** Left: DNT-2A neurons have the vesicular glutamate transporter vGlut (arrows). Right: Colocalization between *Dop2RLex>AopCD8-GFP* and *DNT2Gal4>UASCD8-RFP* in cell bodies of DNT-2A neurons (arrows). **(F)** Terminals of dopaminergic neurons (*TH>mCD8GFP*) abut and overlap those of DNT-2A neurons (*DNT2>CD8-RFP*, magenta), arrows; magnified projections on the right. **(G)** Relative projections of DNT-2 (magenta) and DAL (green) neurons, showing overlapping arborisations at SMP (right). **(H)** *Toll-6>FlyBow1.1* is expressed in Kenyon cells, PPL1, PPL2 and PAM DANs, as revealed by co-localization with anti-TH. **(I)** *kek-6>FlyBow1.1* co-localises with TH in MB vertical lobes, dopaminergic PALs, VUMs, PPL1, PPM2 and PPM3. **(J)** Illustration of neurons expressing DNT-2 (magenta) and its receptors, including KCs, DAN and DAL neurons**. (K)** *kek-6>MCFO* clones in DAL neurons. SMP: superior medial protocerebrum, PRW:

Prow, FLA: Flange, SOG: sub-aesophageal ganglion. Scale bars: (A-C, F-left, G-left, H, I,L-left,K) 50µm; (L-right) 30µm; (D,E,F-right) 25µm.

Figure 2 DNT-2 neurons are functionally connected to dopaminergic neurons

(A) TransTango revealed out-puts of DNT-2 neurons. All neurons express *TransTango* and expression of the TransTango ligand in DNT-2 neurons identified DNT-2 out-puts with Tomato (anti-DsRed). TransTango identified as DNT-2 outputs KC $\alpha'\beta'$ MB lobes (anterior brain, arrow, **top left**); Kenyon and possibly DAN cell bodies (posterior, arrows **top right**); DAL neurons **(bottom left,** arrows) and the dorsal layer of the fan shaped body **(bottom right,** arrow). See also Supplementary Figure S3 for further controls. **(B)** BAcTrace tests connectivity to a candidate neuron input visualised with *LexAop>sybGFP* by driving the expression of a ligand from *DNT-2GAL4* that will activate *QUASTomato* in the candidate input neuron [81]. Candidate PAM neurons visualised at SMP with GFP (green): Control: *R58E02LexA>BAcTrace 806*, no *GAL4*. Test: *R58E02LexA, DNT-2GAL4>BAcTrace 806* revealed PAMs are inputs of DNT-2A neurons at SMP (Tomato, bottom). Magenta shows QUAS-Tomato. **(C)** Optogenetic activation of DNT-2 neurons with *UAS-CsChrimson* excited PAM neurons, revealed with the Ca^{2+} reporter GCaMP6s *(DNT-2>CsChrimson, R58E02LexA>GCaMP6s)* in PAM projections at MB γ lobes. Ratiometric colouring, ROI shown in dashed lines. Average traces are shown for stimulated brains, with retinal (red) and no retinal controls (grey). **(D)** qRT-PCR showing that TH mRNA levels increased with DNT-2 over-expression at 30°C *(tubGAL80^{ts}, DNT-2>DNT-2FL).* One way ANOVA, P=0.0085; post-doc Dunnett's multiple comparison test**. (E)** FRET cAMP probe Epac1 revealed that *DNT-2>Dop2R-RNAi* knockdown decreased YFP/CFP ratio over time in DNT-2A neurons, meaning that cAMP levels increased. Two-way ANOVA, genotype factor p<0.0001, time factor p<0.0001; post-doc Dunnett's. **(F)** Summary: DNT-2 neurons and DANs are functionally connected and modulate each other. Top: DNT-2 can induce *TH* expression. Bottom: DNT-2 stimulates Dopamine production in DANs, followed by negative feedback from DANs to DNT-2 neurons. TH: tyrosine hydroxylase. Scale bars: (A) 50µm; (B) 30µm; (E) 20µm. P values over graphs in (C,E) refer to group analyses; stars

indicate multiple comparisons tests. *p<0.05,**p<0.01, ***p<0.001. For sample sizes and further statistical details, see Supplementary Table S2.

Figure 3 DNT-2 and Toll-6 maintain PAM neuron survival in the developing and adult brain.

(A) Illustration of PAM neuronal cell bodies and experimental temporal profile. DANs are shown in green, DNT-2A neurons in magenta and MB in dark grey. The left hemisphere shows the anterior brain with PAL and PAM DAN neurons (green) and DNT-2 neurons (magenta); the right shows the posterior brain, with the calyx and other DAN neurons (PPM1, PPM2, PPM3, PPL1, PPL2, green). **(B-D)** Fruit-flies were kept constantly at 25°C, from development to adult. Analyses done in adult brains**. (B)** *DNT-2^{37}/DNT-2^{18}* mutants had fewer histone-YFP+ labelled PAM neurons (*THGAL4, R58E02-GAL4>hisYFP).* Un-paired Student t-test. **(C)** *Toll-6* RNAi knock-down in all DANs (*THGAL4, R58E02-GAL4>hisYFP, Toll-6 RNAi)* reduced Histone-YFP+ labelled PAM cell number. Un-paired Student t-test. **(D)** *DNT-2^{37}/DNT-2^{18}* mutants had fewer PAMs stained with anti-TH antibodies. Over-expressing *Toll-6^{CY}* in DANs (*THGAL4, R58E02 GAL4>hisYFP, Toll-6^{CY}*) rescued TH+ PAM neurons in *DNT-2^{37}/DNT-2^{18}* mutants, demonstrating that DNT-2 functions via Toll-6 to maintain PAM cell survival. Welch ANOVA p<0.0001, post-hoc Dunnett test. **(E-H)** Adult specific restricted over-expression or knock-down at 30°C, using the temperature sensitive GAL4 repressor *tubGAL80^{ts}*. **(E)** Adult specific *DNT-2* RNAi knockdown in DNT-2 neurons decreased Tomato+ PAM cell number (*tubGAL80^{ts}, R58E02-LexA, DNT-2 GAL4>LexAOP-Tomato, UAS DNT-2-RNAi*). Un-paired Student t-test, p= 0.005. **(F)** Adult specific *Toll-6* RNAi knock-down in *Toll-6^{31}* heterozygous mutant flies in DANs, reduced Histone-YFP+ PAM cell number (*tubGAL80^{ts}; THGAL4, R58E02-GAL4>hisYFP, Toll-6 RNAi/Toll6^{31}*). Un-paired Student t-test. **(G)** PAMs were visualised with anti-TH. Left: *tubGAL80^{ts}, Toll-6>Toll-6-RNAi* knock-down decreased TH+ PAM cell number. Un-paired Student t-test. Right: *tubGAL80^{ts}, DNT-2>DNT-2-RNAi* knock-down decreased TH+ PAM cell number. Kruskal-Wallis ANOVA, p=0.0001, post-hoc Dunn's test. **(H)** Adult-specific *tubGAL80^{ts}, DNT-2>DNT-2RNAi* knock-down increased the number of apoptotic cells in the brain labelled with anti-DCP-1. Dcp-1+ cells co-localise with anti-TH at least in PAM clusters. One Way ANOVA, p<0.0001, post-doc Bonferroni's multiple comparisons test. DANs>histone-YFP: all dopaminergic neurons expressing histone-

YFP, genotype: *THGal4 R58E02Gal4>UAS-histoneYFP*. *PAMsLexA>tomato*: restricted to PAM DANs: *R58E02LexA>LexAop-nlstdTomato.* Controls: *GAL4* drivers crossed to wild-type Canton-S. Scale bars: (B-G) 30µm; (H) 20µm. Graphs show box-plots around the median. P values over graphs in (D, G right, H) refer to group analyses; stars indicate multiple comparisons tests. *p<0.05, **p<0.01, ***p<0.001. For further genotypes, sample sizes and statistical details, see Supplementary Table S2.

Figure 4 DNT-2, Toll-6 and Kek-6 are required for arborisations and synapse formation in development and in the adult. (A-F) Fruit-flies were kept constantly at 25°C. **(A)** *Toll-6* RNAi knockdown in PAM β2β'2 neurons (*MB301B>FB1.1, Toll-6-RNAi*) decreased dendrite complexity. Un-paired Student t-test. **(B)** Over-expression of cleaved *DNT-2CK* in PAM β2β'2 neurons *(MB301B>CD8-GFP, DNT-2CK)* increased dendrite complexity. Un-paired Student t-test. **(C)** Illustration showing the ROIs (dashed lines) used for the analyses, corresponding to dendrites of PAM and DAL neurons and axonal terminals of PPL1ped neurons. **(D-E)** PPL1ped axonal misrouting was visualised with *split-GAL4 MB320CGal4>FlyBow1.1.* Images show PPL1-γped neurons and some PPL1-α2α'2. **(D,D')** RNAi knock-down of *Toll-6, kek-6* or both (e.g. *MB320CGal4>FlyBow1.1, Toll-6RNAi)* in PPL1-γped neurons caused axonal terminal misrouting (arrows). **(D')** Higher magnification of **(D**, dotted squares**)**. Chi-square for group analysis: p = 0.0224, and multiple comparisons Bonferroni correction control vs *Toll-6RNAi* p<0.01; vs *kek-6RNAi* p<0.05; vs *Toll-6RNAi kek-6RNAi* p<0.01, see Table S2**. (E)** PPL1 misrouting was also induced by over-expressed *DNT-2CK* or *DNT-2FL* (e.g. *MB320CGal4>FlyBow1.1, DNT-2FL)*. Chi-square for group analysis: p<0.05, Bonferroni correction control vs *DNT-2CK* ns, vs *DNT-2FL* *p<0.05, see Table S2. **(F-H)** DAL SLP dendrites visualised with G0431GAL4>UAS-Homer-GCaMP6.0 and anti-GFP antibodies. **(F)** *DNT-2^{37}/DNT-2^{18}* mutants had reduced DAL dendrite complexity (terminal points, Student t test), size (dendrite length, Student t test), number of synapses (No. PSD, Student t test) and synapse density (PSD/total dendrite length, Student t test), and increased PSD volume (Mann Whitney U test). (Genotype: *DNT-2^{18} G0431GAL4>UAS-Homer-GCaMP6.0, DNT-2^{37}*). **(G,H)** Adult specific RNAi knock-down or over-expression in DAL neurons using *tubGAL80^{ts}***. (G**) Over-expression of *DNT-2CK* or *DNT-2FL* increased dendrite complexity (branch points, One Way ANOVA

p=0.0102, post-hoc Dunnett test), did not alter PSD density (One Way ANOVA p=0.0494, post-hoc Dunnett test, all comparisons n.s.) and decreased PSD volume (Kruskal Wallis ANOVA p<0.0001, post-hoc Dunn test). (Genotypes: e.g. *tubGAL80^{ts}, G0431GAL4>UAS-Homer-GCaMP6, DNT-2FL*). **(H)** DAL dendrites with Homer+ post-synaptic densities (PSD) (with overlaid rendering) showing that RNAi knock-down of *Toll-6* or both *Toll-6 kek-6* decreased Homer+ PSD number and synapse density and increased PSD volume. (Genotypes: e.g. *G0431GAL4>UAS-Homer-GCaMP6, Toll-6RNAi)*. Branch points: One way ANOVA p = 0.8606 (ns). No. Homer+ PSD: One way ANOVA p <0.001, post-hoc Dunnett. PSD Density: One way ANOVA p<0.01, post-hoc Dunnett. PSD volume: One way ANOVA p<0.0001, post-hoc Dunnett. Graphs show box-plots around the median or dots plots (PSD volume). P values over graphs in **(G,H)** refer to group analyses; asterisks indicate multiple comparisons tests to a fixed control in (grey). *p<0.05, **p<0.01, ***p<0.001, ****p<0.0001. Scale bars: (A,B,D) 30µm; (D', E,F,G,H) 20µm. For genotypes, sample sizes and statistical details, see Supplementary Table S2.

Figure 5 Neuronal activity induced synapse remodelling depends on DNT-2, Toll-6 and Kek-6. (A) Thermogenetic neuronal activation of DAL neurons with TrpA1 at 30°C after raising flies at 18°C, visualised in the SLP dendrite with Homer-GCaMP and anti-GFP antibodies (*G0431>homer-GCAMP, TrpA1)*. DAL neuronal activity decreased dendrite complexity (terminal points, Mann Whitney U-test) and size (dendrite length, Unpaired Student t test), it did not change synapse number (No. PSD, Unpaired Student t. ns) nor PSD volume (Mann Whitney U, ns), but it increased synapse density (No. PSD/dendrite Length: Mann Whitney-U test). **(B)** Compared to control *DNT-2^{37}/DNT-2^{18}* mutants kept at 18°C, neuronal thermo-activation of DAL neurons at 30°C in *DNT-2^{37}/DNT-2^{18}* mutants decreased terminal points (Unpaired Student t test), did not alter dendrite size (total length, Student t ns), number of synapses (PSDs, Unpaired Student t ns) nor synapse density (PSDs/total dendrite length, Mann Whitney U ns), meaning that synaptic remodelling normally caused by neuronal activity did not occur in *DNT-2^{37}/DNT-2^{18}* mutants. In *DNT-2^{37}/DNT-2^{18}* mutants, PSD volume increased with activity (Mann Whitney U test). (Genotype: *G0431GAL4 UASTrpA1/UASHomer-GCaMP; DNT-2^{37}/DNT-2^{18}*). **(C)** Adult specific RNAi knock-down of *Toll-6* and *kek-6*

reduced PSD number and synapse density and it increased PSD volume. Terminal Points: Unpaired Student t ns. Dendrite length: Unpaired Student t ns. No. PSDs: Unpaired Student t. Synapse density (No. PSDs/dendrite length): Unpaired Student t; PSD volume: Mann Whitney U. (Genotype: *G0431 GAL4 UASTrpA1/UASkek6RNAi UAS-Homer-GCaMP; UASToll-6RNAi/tubGAL80^{ts}*). Graphs show box-plots around the median, except for PSD volume data that are dot plots. *p<0.05, **p<0.01, ***p<0.001, ****p<0.0001; ns: not significantly different from control. Scale bars: 30µm. For Genotypes, sample sizes and statistical details, see Supplementary Table S2.

Figure 6 DNT-2 neuron activation and DNT-2 over-expression induced synaptogenesis. (A) Thermo-activation of DNT-2 neurons at 30°C altered DNT-2 arborisations, here showing an example with smaller dendrites and enlarged axonal arbours (magenta shows 3D-rendering of axonal arborisation done with Imaris, merged with raw image in green). (Genotype: *DNT-2>FlyBow1.1, TrpA1*). **(B)** Thermogenetic activation of DNT-2 neurons increased the number of Homer+ PSDs in DNT-2 neurons, at SMP (*DNT-2>Homer-GCAMP3, TrpA1*, anti-GFP). Test at 30°C 24h: Unpaired Student t test. See Table S2. **(C)** Thermogenetic activation of DNT-2 neurons induced synaptogenesis in PAM target neurons at SMP, but not at MB lobe. (Genotype: *PAM(R58E02)LexA/LexAOP-sytGCaMP; DNT-2GAL4/UASTrpA1*). At SMP: No. Syt+ synapses: Mann Whitney-U; Syt+ synapse volume: Mann Whitney-U. At MB lobe: No. Syt+ synapses: Unpaired Student t ns; Syt+ synapse volume: Mann Whitney-U ns. **(D)** Over-expression of DNT-2FL in DNT-2 neurons increased synapse volume at SMP dendrite and induced synaptogenesis at MB lobe. (Genotype: *PAM(R58E02)LexA/LexAopSytGcaMP6; DNT-2Gal4/UAS-DNT-2FL*). At SMP: No. Syt+ synapses: Unpaired Student t ns. Syt+ synapse volume: Mann Whitney-U. At MB lobe: No. Syt+ synapses: Unpaired Student t; Syt+ synapse volume: Mann Whitney-U ns. Graphs show box-plots around the median, except for PSD volume data that are dot plots. *p<0.05, ****p<0.0001; ns: not significantly different from control. Scale bars: 30µm. For Genotypes, sample sizes, p values and other statistical details, see Supplementary Table S2.

Figure 7 DNT-2-induced circuit plasticity modified dopamine-dependent behaviour. (A) *DNT-2* mutants (left, *DNT-2^{37}/DNT-2^{18}*) and flies with adult-specific RNAi knock-down of *DNT-2* in DNT-2 neurons (right, *tubGAL80^{ts}; DNT-2>DNT-2RNAi*), had impaired climbing. Left Mann Whitney U; Right: One Way ANOV, post-hoc Dunnett. **(B)** Adult-specific *Toll-6* and *kek-6* RNAi knock-down in Toll-6 *(tubGAL80^{ts}; Toll-6>Toll-6RNAi, kek-6RNAi,* left) or PAM (*tubGAL80^{ts}; R58E02>Toll-6RNAi, kek-6RNAi,* right) neurons impaired climbing. Left: Welch ANOVA, post-hoc Dunnett. Right: Welch ANOVA, post-hoc Dunnett. **(C)** The climbing impairment of *DNT-2* mutants could be rescued with the over-expression of *Toll-6^{CY}* in dopaminergic neurons (Rescue genotype: UASToll-6^{CY}/+; DNT-2^{18}*THGAL4 R58E02GAL4/DNT-2^{37}).* Welch ANOVA, post-hoc Dunnett. **(D)** Adult specific over-expression of *Toll-6^{CY}* in DANs increased locomotion in *DNT-2^{37}/DNT-2^{18}* mutants. (Test genotype: *UASToll-6^{CY}/+; DNT-2^{18}THGAL4 R58E02GAL4/DNT-2^{37}*). Walking speed: Kruskal Wallis ANOVA, post-hoc Dunn's. Distance walked: Kruskal Wallis ANOVA, post-hoc Dunn's. Time spent immobile: Kruskal Wallis ANOVA, post-hoc Dunn's. **(E)** Adult specific *DNT-2FL* overexpression in DNT-2 neurons increased fruit-fly locomotion speed in an open arena at 30°C (see also Supplementary Figure S6A for further controls). (Test genotype: *tubGAL80^{ts}, DNT-2>DNT-2FL*) Kruskal-Wallis, post-hoc Dunn's test. **(F)** Thermogenetic activation of DNT-2 neurons at 30°C *(DNT-2>TrpA1)* increased fruit-fly locomotion speed. (See also Supplementary Figure S6B for further controls). One Way ANOVA p<0.0001, post-hoc Dunnett's test**. (G)** Over-expression of *DNT-2-FL* in DNT-2 neurons increased long-term memory. (Test genotype: *tubGAL80^{ts}, DNT-2>DNT-2FL*). Left: 23°C controls: One Way ANOVA p=0.8006. Right 30°C: One Way ANOVA, post-hoc Dunnett's test. Graphs show box-plots around the median, under also dot plots. P values over graphs refer to group analyses; asterisks indicate multiple comparisons tests. *p<0.05, **p<0.01, ***p<0.001, ****p<0.0001; ns: not significantly different from control. For further genotypes, sample sizes, p values and other statistical details, see Supplementary Table S2.

SUPPLEMENTAL INFORMATION

Supplementary Figure S1 Identification of neurotransmitter type for DNT-2A neurons. (A, B) Anterior DNT-2A neurons projecting at SMP are not dopaminergic, as there was no co-localisation between

DNT-2>histoneYFP and anti-TH in the anterior brain **(A),** and there was no colocalization in other DNT-2+ neurons in the posterior brain either **(B).** Higher magnification of dotted boxes on the right. **(C)** There was no colocalisation with *Dop1R2LexA>CD8::GFP, DNT-2Gal4>CD8::RFP* either. **(D)** DNT-2 neurons are not not serotonergic, as there was no co-localization between *DNT-2>FlyBow1.1* and the serotoninergic neuron marker anti-5HT**. (E)** There are not octopaminergic, as there was no overlap between *TdcLexA>mCD8::GFP and DNT-2Gal4>CD8::RFP*. **(F)** There was no overlap between *DNT-2Gal4>histoneYFP* and the cholinergic neuron marker anti-ChAT4b1. **(G,H)** Anterior DNT-2A neurons are not GABAergic, but lateral DNT-2 neurons are, as visualised with *DNT-2>CD8-RFP, GADLexA>CD8-GFP*. Scale bars: (A,B left) 50µm; (C-H) 20 µm. For further genotypes and sample sizes, see Supplementary Table S2.

Supplementary Figure S2 Identification of *Toll-6* and *kek-6* expressing neurons. (A) *Toll-6Gal4, MB247-Gal80>UASFlyBow1.1* and *kek-6Gal4, MB247-Gal80>UASFlyBow1.1* revealed Toll-6+ and Kek-6+ projections on MB γ2α'1. **(B)** *R25D01LexA>CD8GFP, kek6-Gal4>CD8RFP* overlapped in MB γ2α'1. **(C)** *R14C08LexA>CD8GFP, Toll-6Gal4>CD8-RFP13* revealed co-localization in MBON-M4/M6 cell bodies. **(D,E)** Co-localisation of *Toll-6>Histone-YFP* and *kek-6>HistoneYFP* with TH in PPL1 neurons. **(F)** Number of PAM and PPL1 neurons expressing *Tolls* and *kek-6,* revealed from published RNAseq data (Scope, see also Table S1). **(G, H)** Toll-6 and kek-6 are expressed in DAL neurons. **(G)** DAL neurons express *Toll-6,* as revealed by co-localization between *DAL-LexA (VT49239-LexA)>mCD8-GFP* and *Toll-6GAL4>mCD8-RFP*. **(H)** DAL neurons express *kek-6*, as revealed by colocalization between *DAL-LexA (VT49239-LexA)>mCD8-GFP* and *kek6GAL4>mCD8RFP*. **(I, J)** Toll-6 and kek-6 are expressed in MB neurons. **(I)** *Toll-6>MCFO* clones reveal expression at least in MB neurons γ medial (γm), αβcore (αβc) and αβsurface (αβs). **(K)** *kek-6>MCFO* clones reveal expression at least in MB Kenyon cells αβα'β'γ formed and MB γ2α'1 and α2α'2 and PPL1-γ2α'1 and PPL1-α2α'2. Scale bars: (B, H) 50µm; (A,C,D,G, I, J) 30µm. For further genotypes and sample sizes, see Supplementary Table S2.

Supplementary Figure S3 **TransTango connectivity controls. (A)** *UAS-TransTango/+* control, showing background GFP expression in mushroom bodies and Tomato+ signal in sub-aesophageal ganglion (SOG). **(B)** *DNT-2GAL4>UAS-TransTango*, revealing the GFP+ DNT-2 neurons and Tomato+ signal in DNT-2 neurons. TransTango also reveals what appears to be feedback connections between DNT-2 neurons from SMP to PRW (arrow). These are controls for Figure 3A. Scale bars: (A,B) 50µm. For further genotypes and sample sizes, see Supplementary Table S2.

Supplementary Figure S4 **Activity controls**. **(A)** Controls for thermogenetic neuronal activation of DAL neurons, whereby control flies with and without TrpA1 were raised at 18°C and kept constantly at 18°C, see Figure 5A. DAL-SLP dendrites were visualised with Homer-GCaMP and anti-GFP antibodies (*G0431>homer-GCAMP* and *G0431>homer-GCAMP, TrpA1* at 18°C). Terminal points: Man Whitney U test: p=0.0257. Dendrite length: Student t test ns. No of PSD: Student t test p=0.4427. Synapse density (PSD/dendrite length): Mann Whitney U test ns. PSD volume: Mann Whitney U test ns. **(B)** Control of DNT-2FL-GFP production, at 18°C, see Figure 6B. DNT-2 bidirectional arborisation at SMP was visualised with Homer-GCaMP and anti-GFP antibodies (*DNT-21>homer-GCAMP* and *DNT-2>homer-GCAMP, TrpA1* at 18°C). Unpaired Student t-test, ns. Scale bars: (A,B) 30µm. For further genotypes, sample sizes, p values and other statistical details see Supplementary Table S2.

Supplementary Figure S5 **Neuronal activity increased production and cleavage of DNT-2. (A)** Thermogenetic activation of DNT-2 neurons increased the number of DNT-2FLGFP+ vesicles or spots (*DNT-2>DNT-2-FL-GFP*, *TrpA1* with anti-GFP). Control 18°C: Unpaired Student t test, ns. Activation 30°C 24h: Mann Whitney**. (B)** Western blot from fly heads over-expressing DNT-2FL-GFP in DNT-2 neurons showing that neuronal activation with TrpA1 at 30°C increased DNT-2FL-GFP cleavage. **(**Genotype: *DNT-2>TrpA1, DNT-2FL-GFP*). Controls are flies of the same genotype kept constantly at 18°C as well as flies treated also at 30°C but lacking TrpA1. High temperature (30°C) is sufficient to increase fly activity. ***p<0.001. ns= not

significant. For further genotypes, sample sizes, p values and other statistical details see Supplementary Table S2.

Supplementary Figure S6 **Locomotion in open arena controls. (A)** In 18°C controls, GAL80 is on and GAL4 is off, thus there is no adult specific *DNT-2FL* overexpression in DNT-2 neurons in these flies. (Genotype: *tubGAL80ts, DNT-2>DNT-2FL*). Consistently, there was no increase in locomotion speed in an open arena, in flies over-expressing *DNT-2FL* relative to controls, compare also to Figure 7G. Kruskal Wallis ANOVA ns (lower median in *UAS-DNT-2FL/+* control). **(B)** The cation TrpA1 opens at high temperatures (eg 30°C) but remains closed at 18°C. Consistently, there was no effect in locomotion at 18°C in flies of genotype *DNT-2>TrpA1* compared to controls, compare also to 30°C data in Figure 7F. Kruskal Wallis ANOVA ns. For further genotypes, sample sizes, p values and other statistical details see Supplementary Table S2.

Supplementary Figure S7 **Altering *DNT-2* levels induced seizures.** Knock-down or over-expression of *DNT-2* in the adult, using $GAL80^{ts}$. Fruit-flies were reared at 18°C from egg laying to adult eclosion, when they were transferred to 30°C and kept there for 5 days prior to testing**.** To test for seizures, we used the bang-sensitivity test. $DNT2^{37}/DNT2^{18}$ mutant flies (left) and adult *DNT-2* knock-down flies ($tubGal80^{ts}$ *DNT-2Gal4>DNT-2RNAi,* centre) took longer to recover than controls. Over-expression of *DNT-2FL* in DNT-2 neurons ($tubGal80^{ts}$ *DNT-2Gal4>DNT-2FL,* right) increased variability in recovery time. For further genotypes and sample sizes see Supplementary Table S2.

Supplementary Figure S8 **Activation of DNT-2 neurons does not influence memory consolidation.** Flies were bred at 18°C, transferred to 23°C for starvation, trained and moved to 30°C for 6h followed by 23°C for another 18h, until testing 24h post-training; controls were kept at 23°C from starvation on. Control flies of all genotypes could learn, and differences between genotypes were not statistically significant. *DNT-2>TrpA1* flies had better memory than *UAS-TrpA1/+* controls. 23°C control: One Way ANOVA ns. Test 6h

30°C, test LTM at 24h: One Way ANOVA p=0.056, post-hoc Dunnett's test. For further genotypes, sample sizes, p values and other statistical details see Supplementary Table S2.

Table S1 Expression of *Tolls, keks* and Toll downstream adaptors in cells related to DNT-2A neurons. Genes expressed in DNT-2 neurons, their potential and/or experimentally verified inputs and outputs, were identified with a combination of reporters (this work) and data from public single-cell RNAseq databases.

Table S2 Statistical analysis. Table providing full genotypes, sample sizes, statistical tests, multiple comparison corrections and p values.

FIGURE 1 Neurons expressing *DNT-2* and its receptors *Toll-6* and *kek-6* in the adult brain

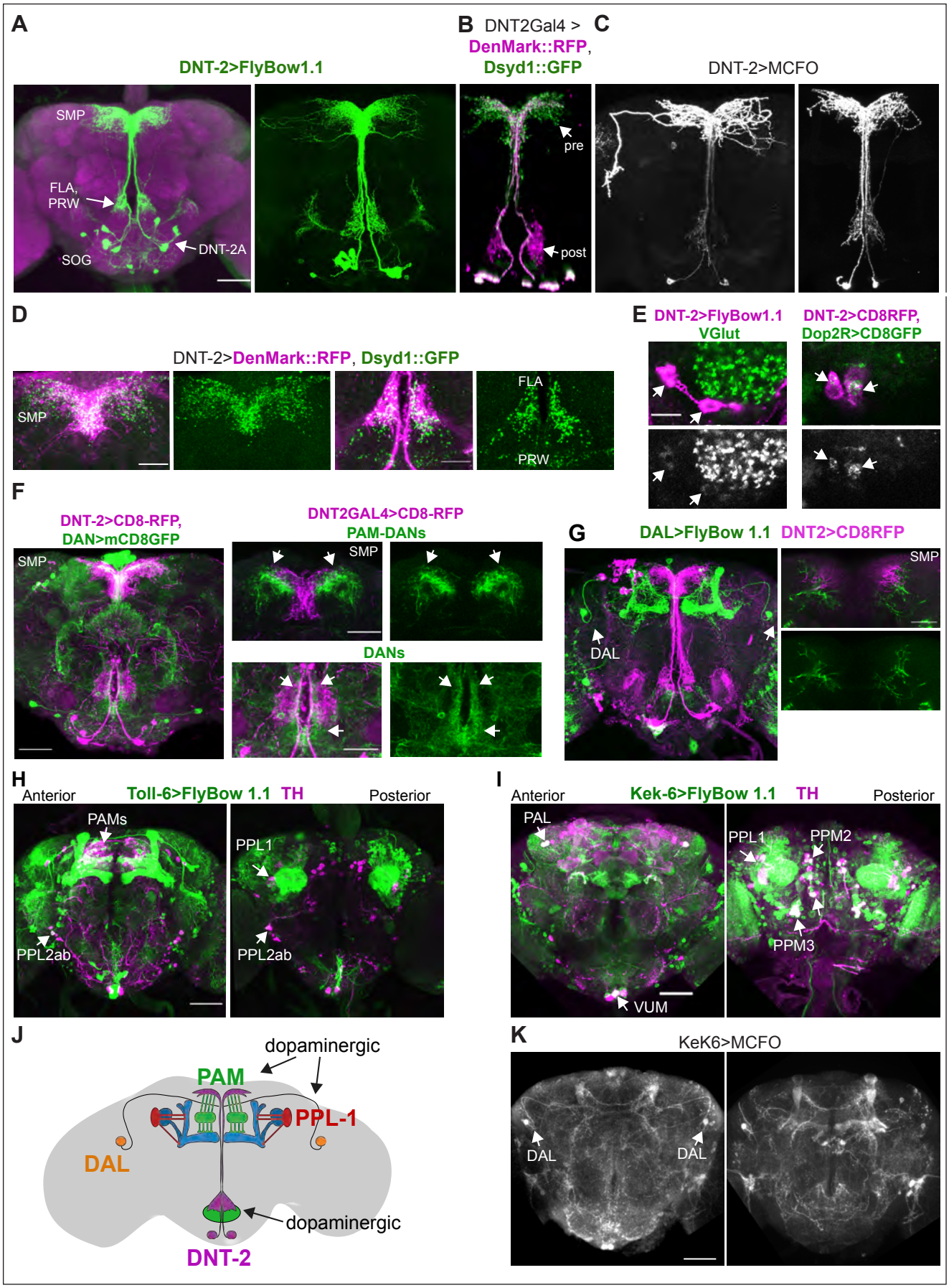

Figure 2 DNT-2 neurons are functionally connected to dopaminergic neurons

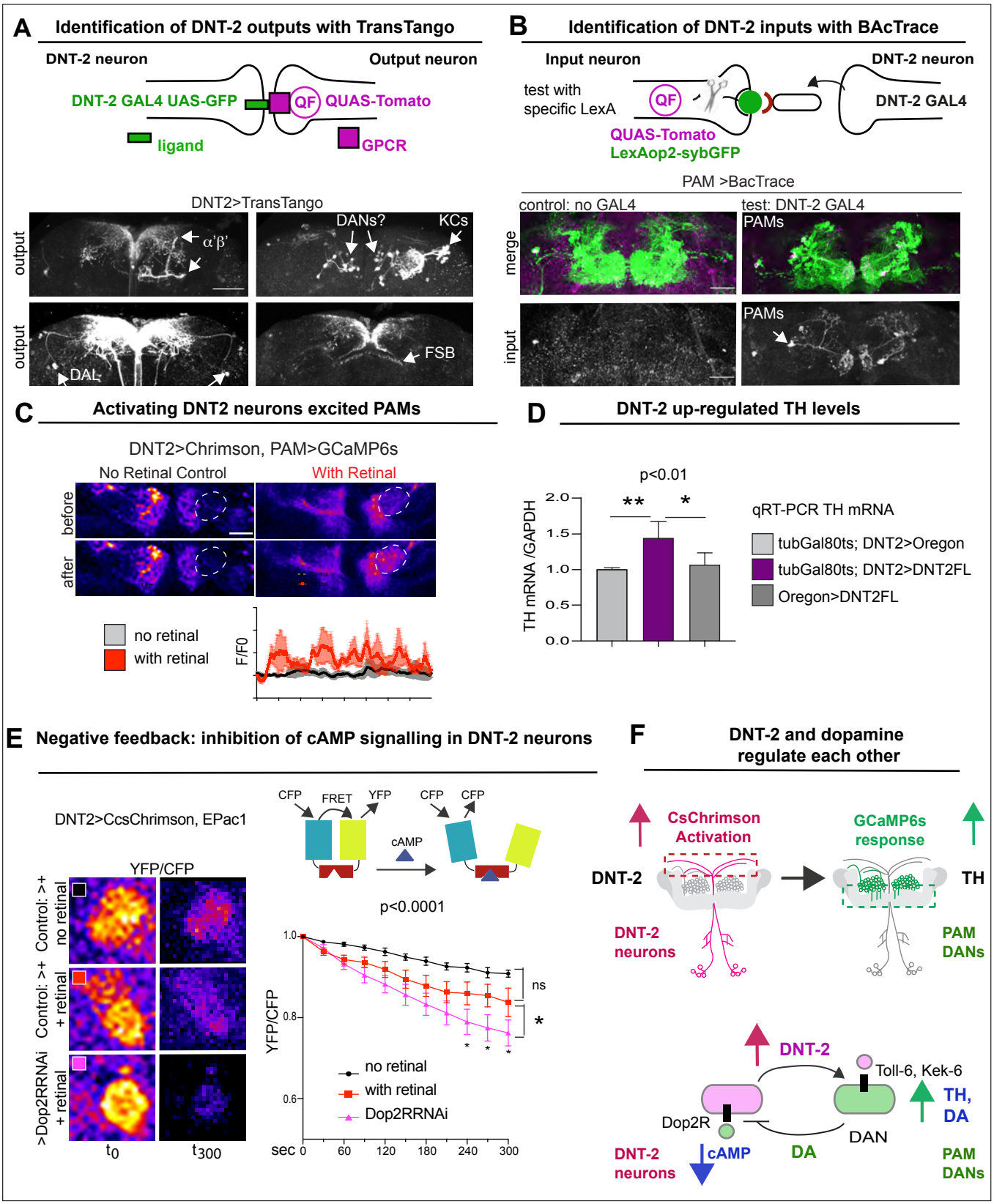

Figure 3 DNT-2 and Toll-6 maintain PAM neuron survival in the developing and adult brain

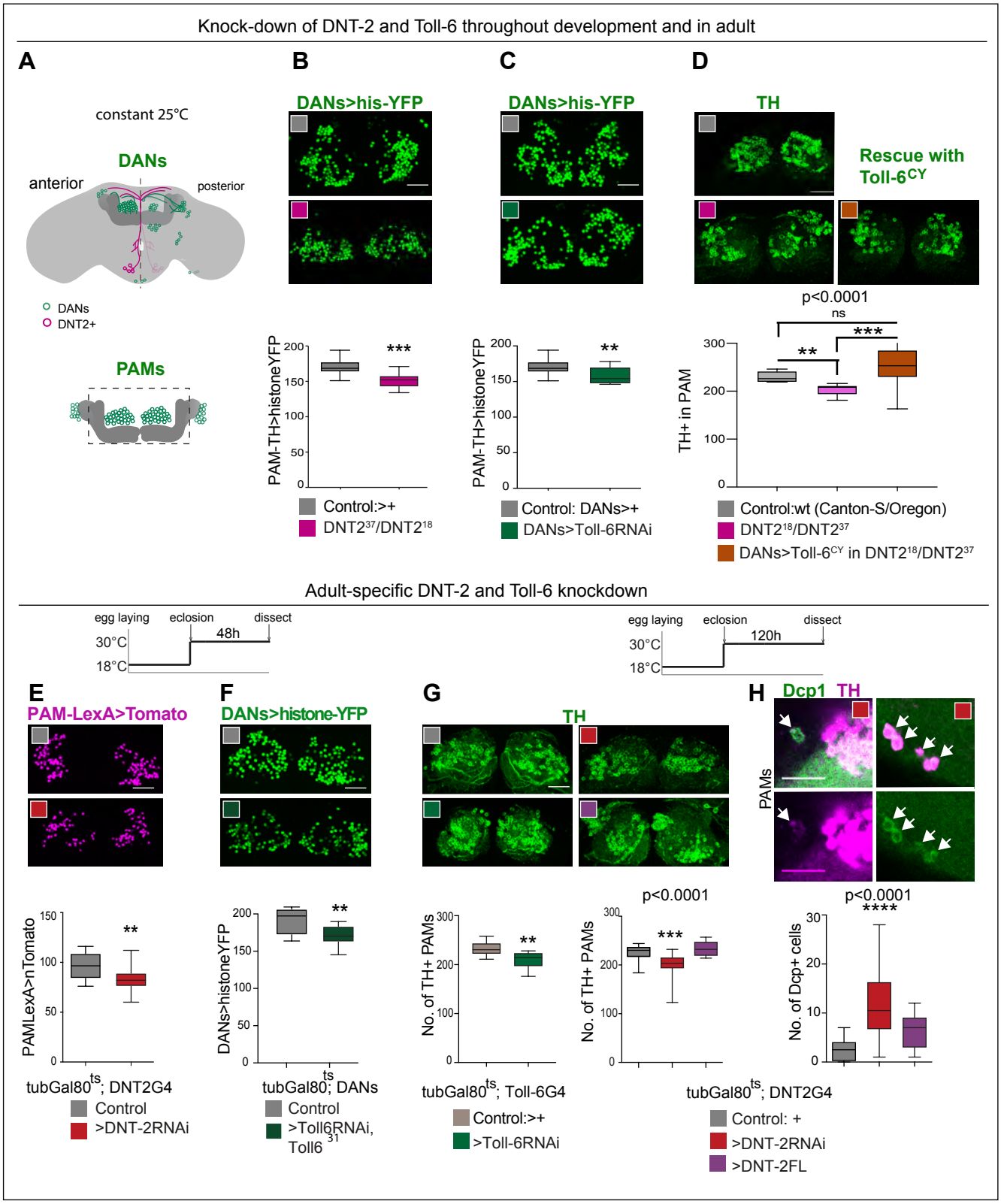

Figure 4 DNT-2, Toll-6 and Kek-6 are required for arborisations and synapse formation in development and in the adult.

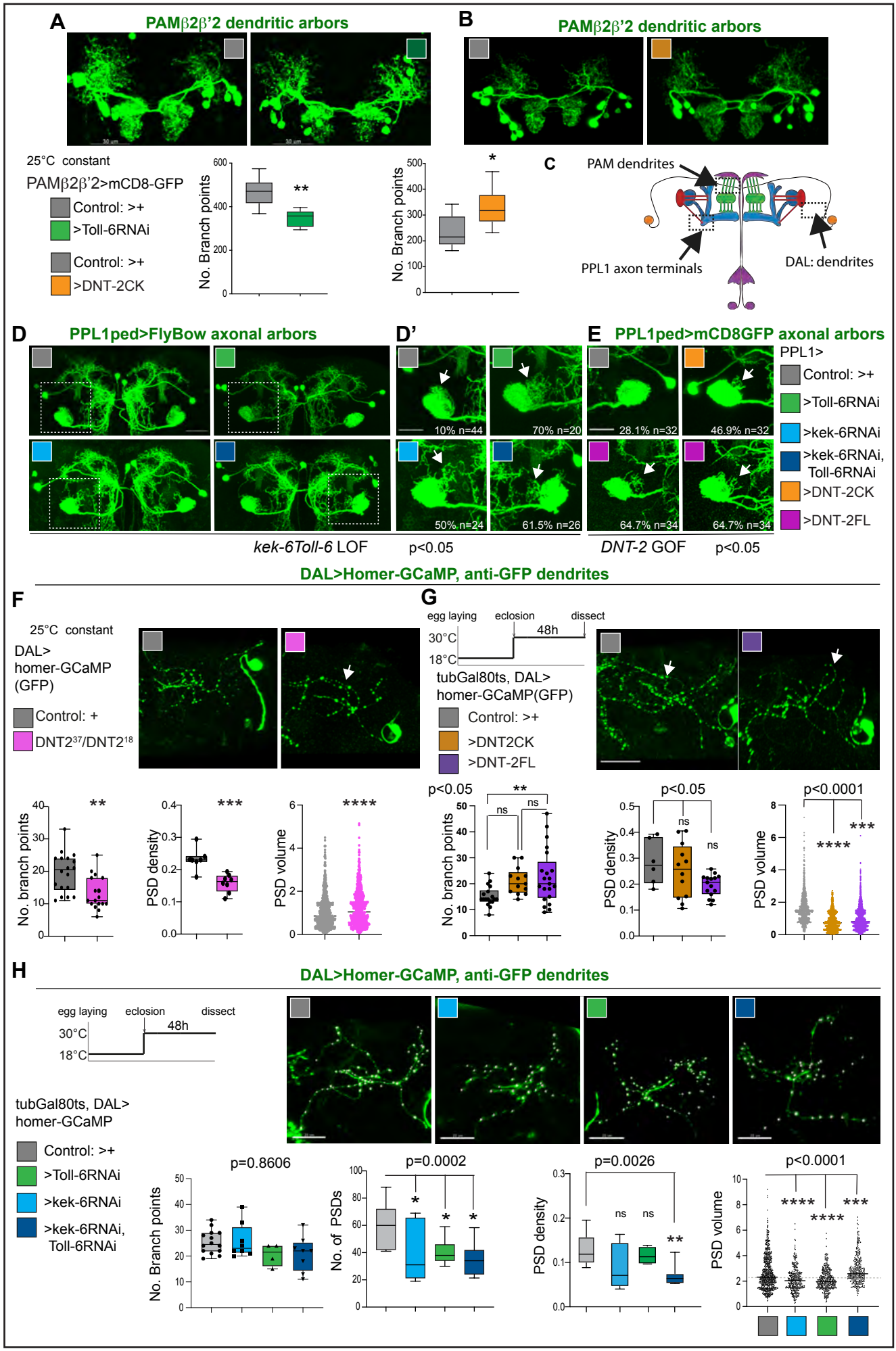

Figure 5 Neuronal activity induced synapse remodelling depended on DNT-2, Toll-6 and kek-6

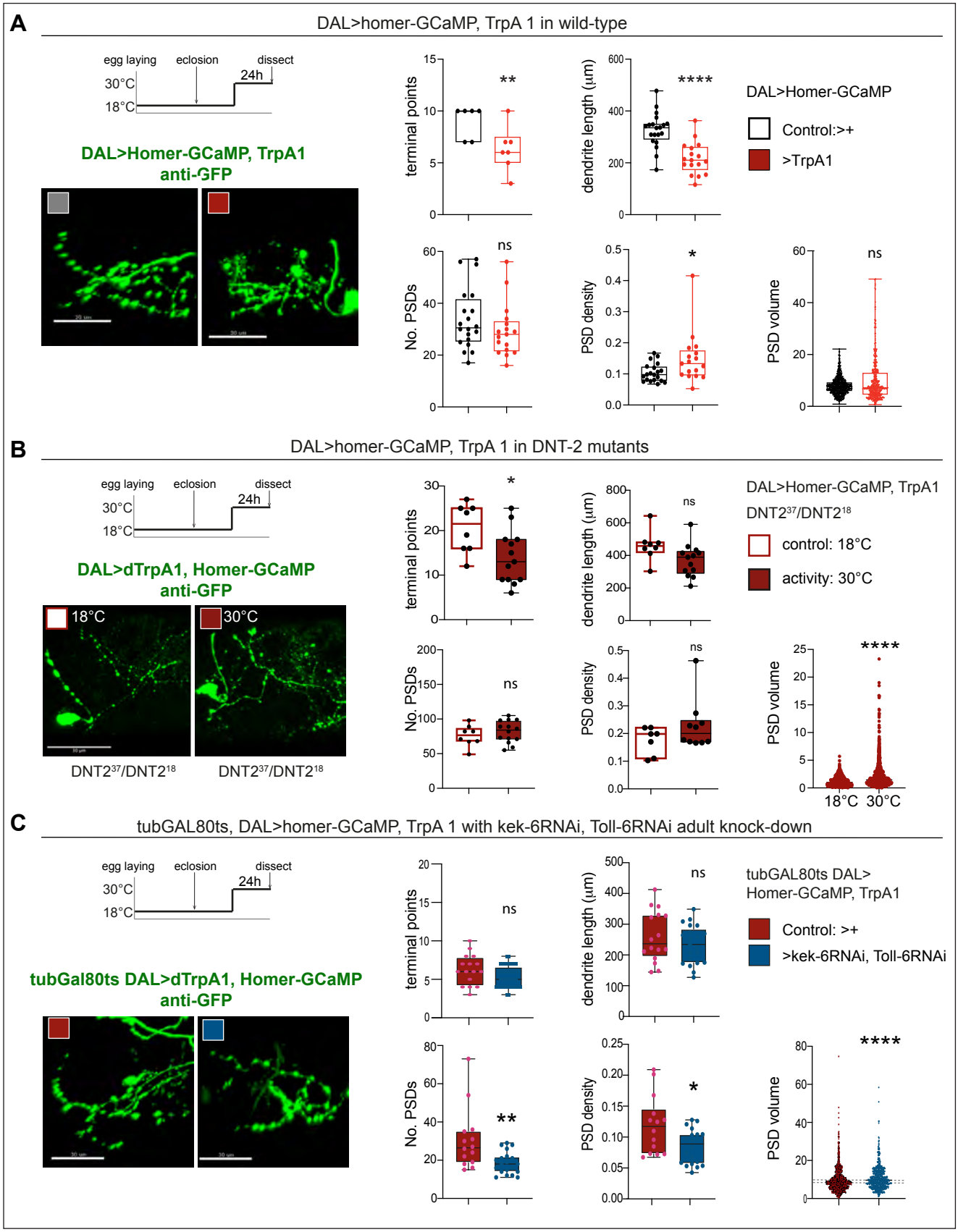

Figure 6 DNT-2 neuron activation and DNT-2 over-expression induce synaptogenesis

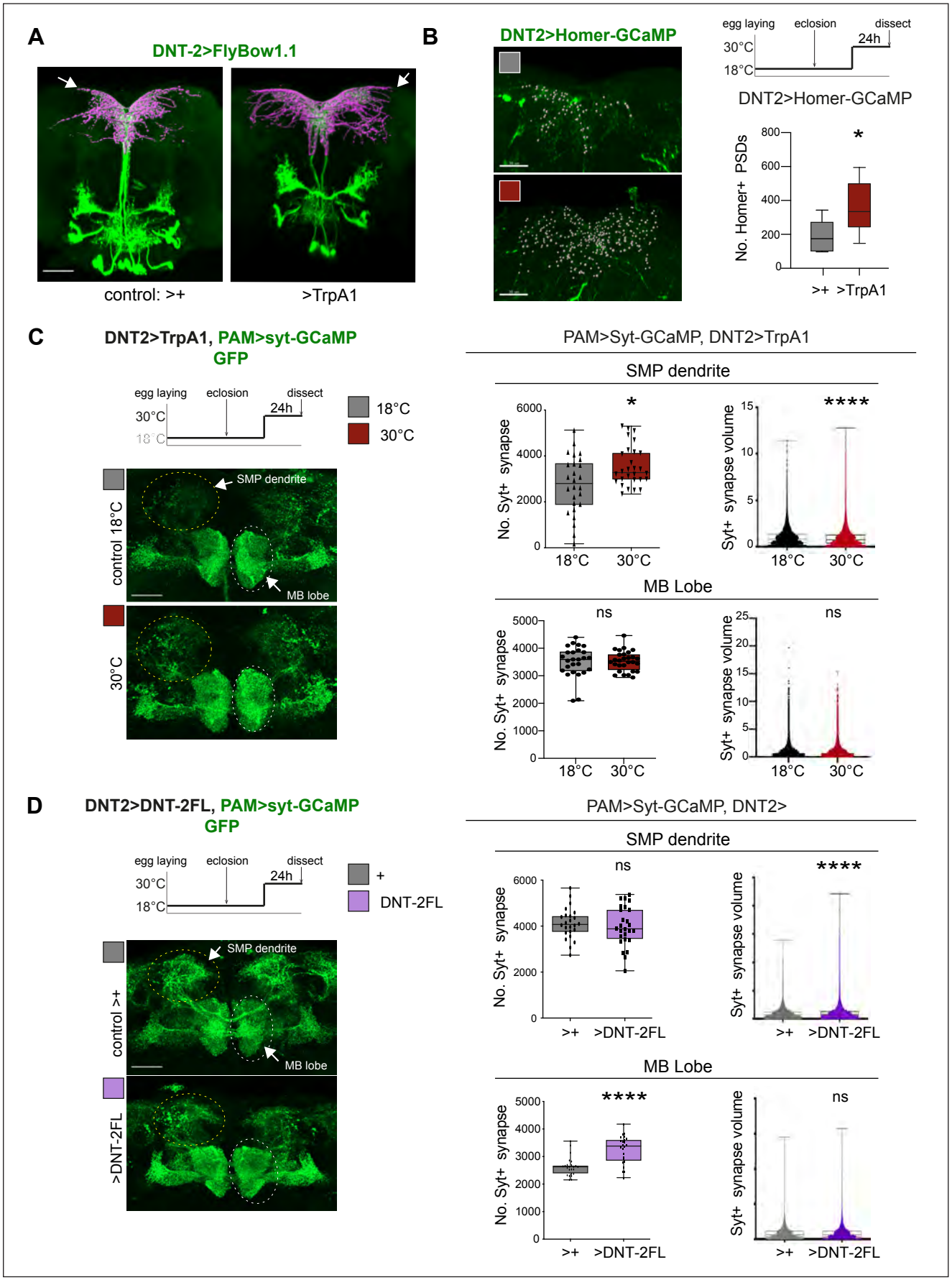
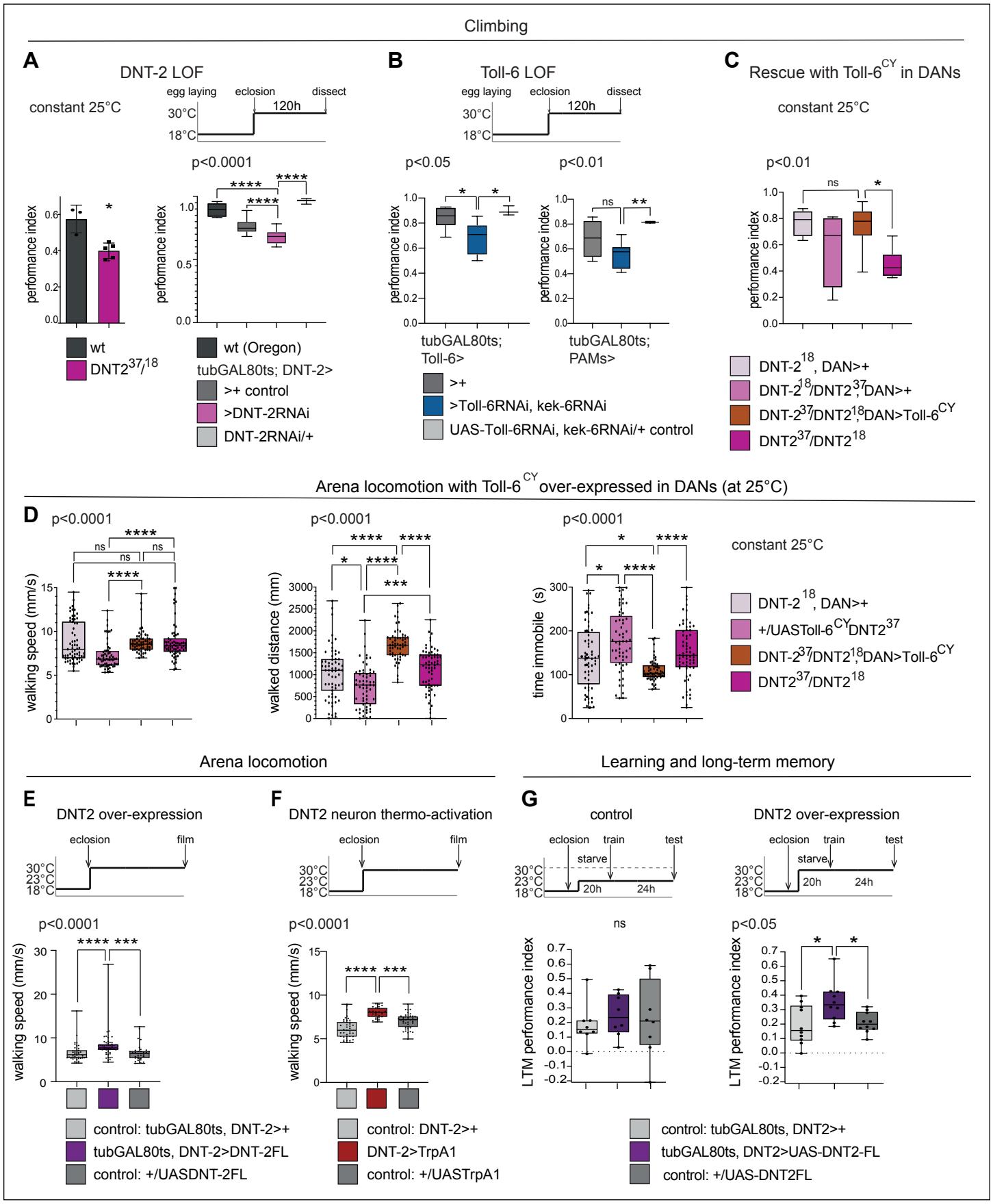
Figure 7 DNT-2-induced circuit plasticity modified dopamine-dependent behaviours.